THE UNIVERSITY OF SOUTHERN MISSISSIPPI

University of Southern Mississippi
School of Ocean Science and Engineering

FINAL REPORT

Monitoring 2019 Bonnet Carré Spillway Impacts

Principal Investigator

Read Hendon
University of Southern Mississippi
School of Ocean Science and Engineering
Gulf Coast Research Laboratory
703 East Beach Drive, Ocean Springs, MS 39564
read.hendon@usm.edu

Co Principal Investigators

Jerry Wiggert
USM-SOSE Division of Marine Science
jerry.wiggert@usm.edu

and

Jill Hendon
USM-SOSE Center for Fisheries Research and Development
jill.hendon@usm.edu

Project Period: June 1, 2019 – August 31, 2019

INTRODUCTION

In response to the multiple and extended openings of the Bonnet Carré spillway in 2019, the University of Southern Mississippi (USM) conducted ecological sampling in the Mississippi Sound and adjacent waters, conducted sample analyses, and provided weekly updates of findings in an effort to better understand the impacts of the freshwater diversion on Mississippi's coastal and marine resources. The period of performance for this project was June 1, 2019, to August 31, 2019. Weekly updates of monitoring activities were provided by USM to MDMR, and updates were posted to the USM Gulf Coast Research Laboratory website (http://gcrl.usm.edu/news/2019.bonnet.carre.spillway.overview.php), after review and approval. This document represents the final activity report summarizing the completed work.

Specific focus areas of this project included:

1. Water Quality - salinity, dissolved oxygen, temperature, turbidity, nutrients, and source water identification; this component also included analyses for primary production, such as phytoplankton community structure and bacteriology (e.g., chlorophyll-a, *Vibrio* sp., microbial community structure);

2. Remote Sensing and Circulation Modeling - spatio-temporal variability of freshwater plumes and associated sediments, circulation modeling, and atmospheric modeling;

3. Fishery Resources - expanded fishery-independent sampling for blue crabs (via crab trap) and assessment of oyster larvae recruitment (via spat settlement plates); and,

4. Data Synthesis - centralization and QA/QC of all data collected as part of this project; note that termination of this project on August 31, 2019, did not allow for a detailed quantitative assessment of impacts from the spillway opening, as field sampling extended to August 29 and associated laboratory analyses of samples were fast-tracked to meet with August 31 termination date.

Summaries of materials and methods and results are provided for each project component below. Note that figure numbers are not consecutive throughout the report and relate generally to each component (or sub-component) section. Financial data and final invoice have been provided independently by USM's Office of Research Administration.

Component 1: Water Quality

Component Lead Investigator: Stephan Howden
Co-PIs: Adam Boyette, Kevin Dillon, Chris Hayes, Jill Hendon, Scott Milroy, Alan Shiller

Methods

Sixteen fixed stations spanning throughout the Mississippi Sound and just south of the barrier islands were selected to be sampled weekly (Figure 1; Table 1). Two, center console boats (18-22 ft), one deployed in the east and one deployed in the west, conducted sampling at all 16 stations on the same day. Water sampling was conducted during daylight between the hours of 8:00am and 5:00pm. At each site, a surface water (0.5 m below the surface) and a bottom water (0.5 m from the bottom) sample was collected using a 5L WaterMark horizontal polycarbonate water sampler. The water from the sampler then was used to fill specific receptacles for individual analyses. These receptacles were place on ice or in a cool environment (per individual protocol) until they were returned to the laboratory (approximately 2-5 hours post collection). A YSI ProDSS multiparameter sonde instrument was then deployed to obtain a continuous vertical profile of pH, conductivity (µS/cm), temperature (°C), dissolved oxygen (mg/L), and turbidity (FNU) for the entire water column. An 8 inch Secchi disk was also deployed on the shady side of the boat to determine visual turbidity (m).

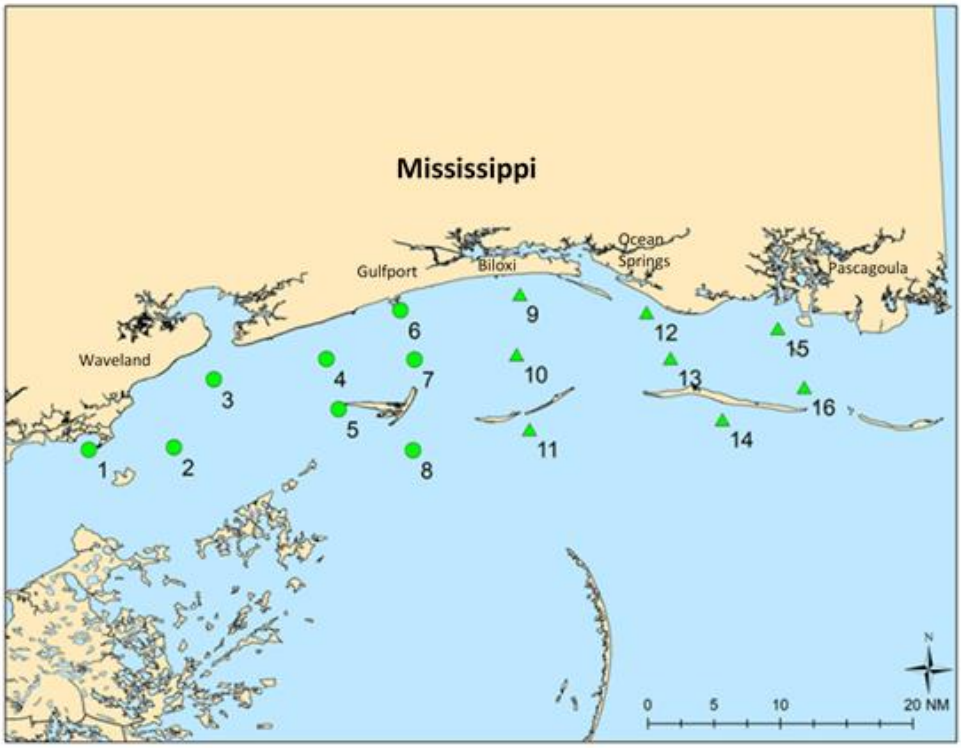

Figure 1. *Map of the waters off of Mississippi. Each green mark represents a fixed station that was routinely sampled. Circle were sampled by a boat in the west, triangles were sampled by a boat in the east.*

Table 1. *Table of station GPS points. Station numbers below correspond to station numbers in Figure 1.*

Station	Latitude (ºN)	Longitude (ºW)
1	30.17230	-89.4752
2	30.17523	-89.3680
3	30.26036	-89.3181
4	30.28605	-89.1765
5	30.22294	-89.1611
6	30.34696	-89.0833
7	30.28531	-89.0657
8	30.17158	-89.0676
9	30.36677	-88.9328
10	30.29118	-88.9372
11	30.19725	-88.9211
12	30.34402	-88.7736
13	30.28678	-88.7435
14	30.20973	-88.6782
15	30.32408	-88.6085
16	30.25009	-88.5755

Results

Twelve water sampling regimes were conducted from June 13 to August 29, 2019. All 16 stations were conducted on the same day except for one week in August. On August 13th stations 4-16 were completed. A thunderstorm over Pass Christian prevented stations 1-3 from being collected. A vessel went out the next day, August 14th, to collect those three stations. The dates of sampling can be found in Table 2.

Table 2. *Dates of sampling. The date and the stations completed are shown in this table. Note that all stations were conducted on the same day except for on August 13th. The missed stations were completed the next day on August 14th.*

Date	Stations Completed
06/13/2019	1-16
06/17/2019	1-16
06/26/2019	1-16
07/02/2019	1-16
07/09/2019	1-16
07/17/2019	1-16
07/25/2019	1-16
08/01/2019	1-16
08/07/2019	1-16
08/13/2019	4-16
08/14/2019	1-3
08/22/2019	1-16
08/29/2019	1-16

Figure 1. *Salinity in Mississippi Sound surface water during Summer 2019 Spillway opening*

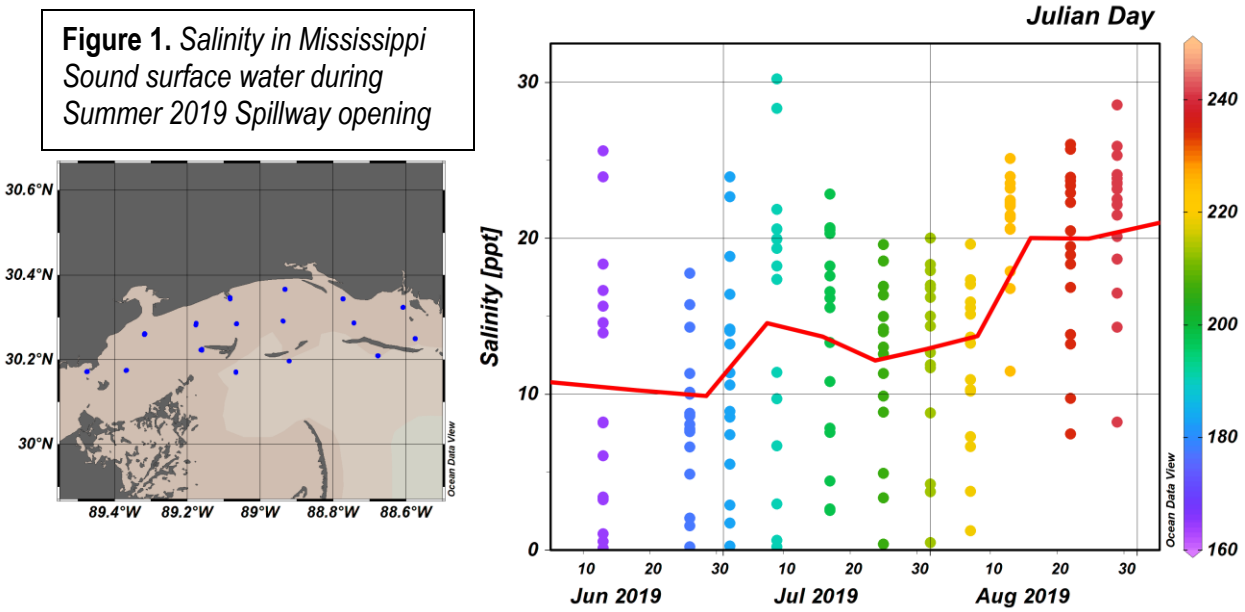

Carbon Parameters (Hayes)

Throughout the observation period, there was a general increase in average salinity in the surface water of the Sound (Fig. 1; red line is the Sound-wide average). Surface water was defined as ~0.5 meter below the sea surface. In particular, by mid-to-late August there were no longer any salinities observed below 5 ppt after the closing of the Bonnet Carré Spillway. Freshwater in the Sound has contributions from Mississippi/Alabama rivers as well as from the Bonnet Carré Spillway. The Spillway (Mississippi River) water is characterized by a much higher alkalinity than the MS/AL rivers. Alkalinity is a measure of the water's ability to neutralize acids. The high salinity, Gulf of Mexico seawater also has a high alkalinity, so the impact of this unique freshwater source can be best seen in the cross-plot of total alkalinity versus salinity below (Fig. 2). In June and early July (Julian days 160-190), there was clearly an influence of freshwater with a higher than normal Alkalinity, seen most obviously at salinities between 2 and 12 ppt.

Figure 2. *Total alkalinity vs. salinity during Summer 2019 Spillway opening*

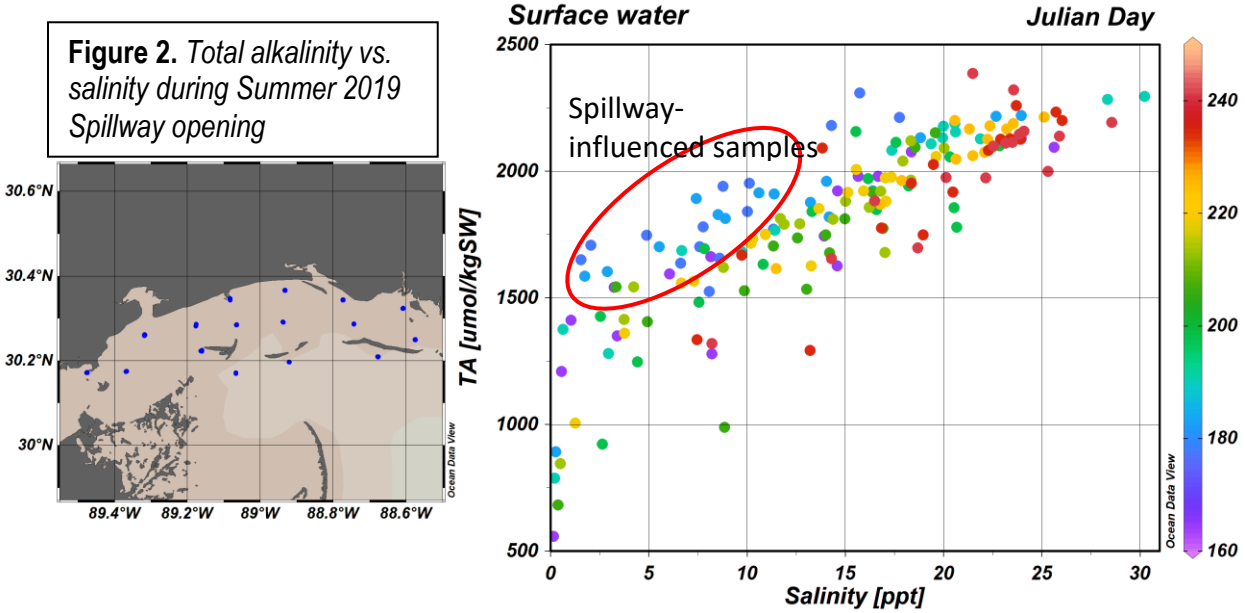

While we clearly see the signature of a higher alkalinity freshwater source, the overall increase in salinity of the Sound seems to dominate the change in the total Alkalinity over time (Fig. 3). Alkalinity also appears to have a general increase throughout the observation period.

Figure 3. *Total alkalinity (TA) in Mississippi Sound surface water during Summer 2019 opening*

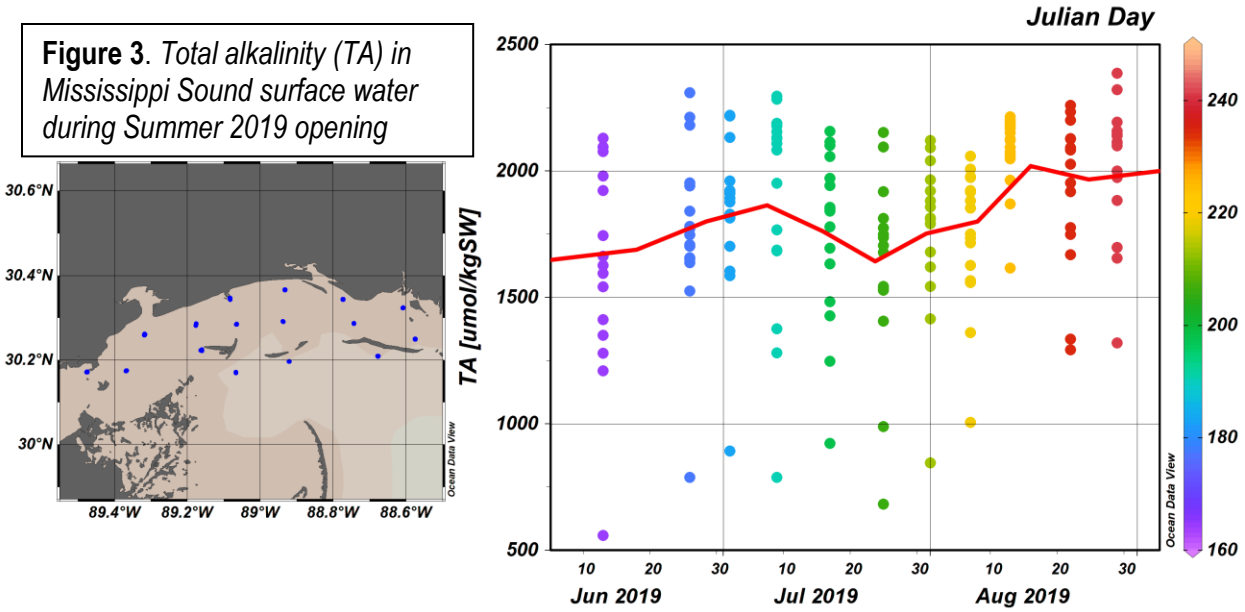

To determine the saturation state of carbonate minerals that shell-making organisms produce, we also measured the total dissolved inorganic carbon (or total CO2, TCO2). From Alkanity and TCO2, we can calculate the saturation state of calcite and aragonite (Omega_cal and Omega_arag). Omega equal to 1 is defined as saturation, Omega < 1 is undersaturated and Omega > 1 is supersaturated. The shells of adult eastern oysters are made out of calcite, while their larvae are known to have thin aragonite shells. In general, lower saturation states (lower omega values) make it more difficult for organisms to make their shells. Mirroring the change in salinity, both saturation state parameters increase throughout the observation period, with much more observations of undersaturation (omega < 1) observed during June-July-early-August than in late August (Fig. 4 & 5).

Figure 4. *Surface calcite saturation state during Summer 2019 Spillway opening*

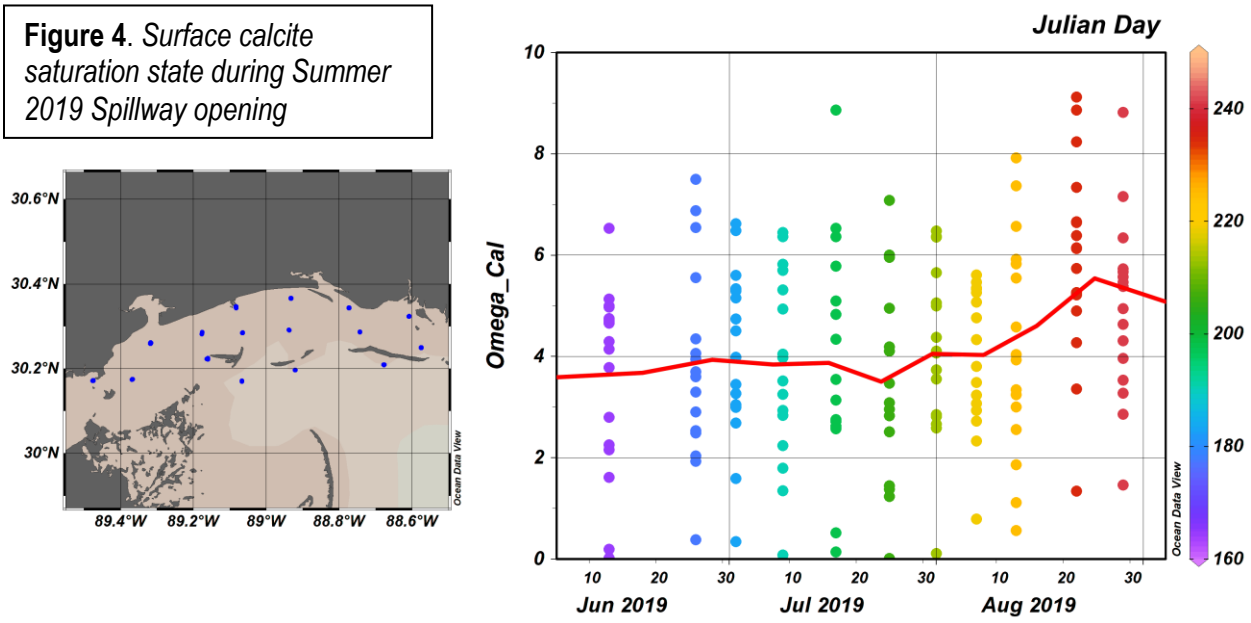

Figure 5. *Surface aragonite saturation state during Summer 2019 Spillway opening*

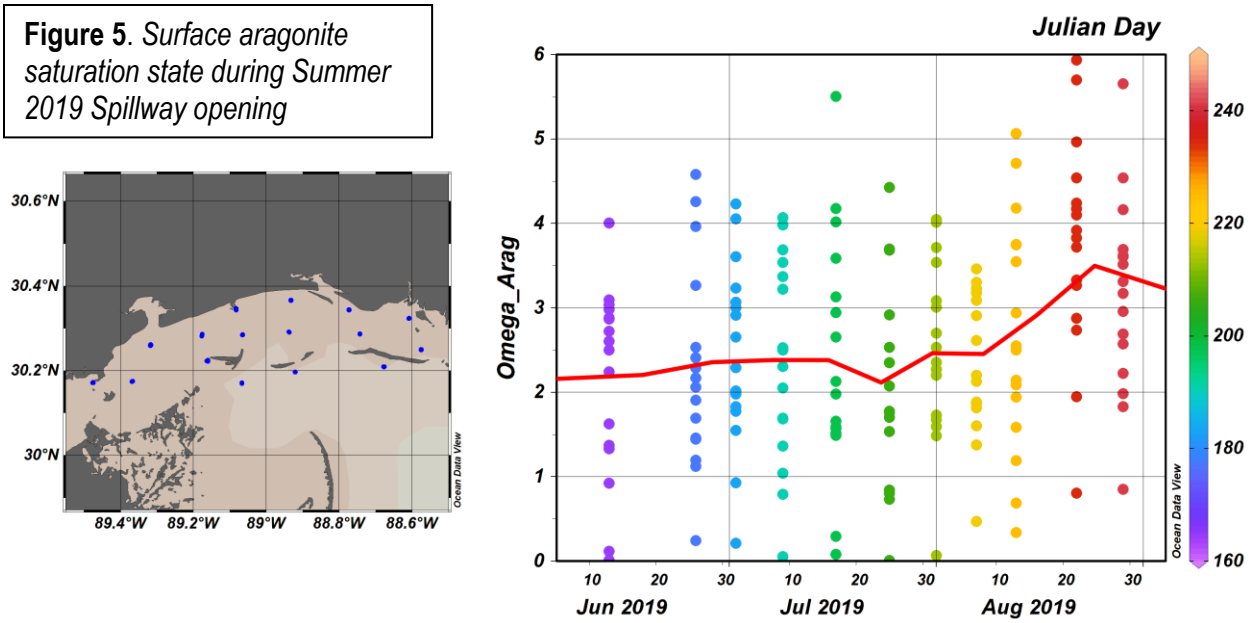

Bottom water at all of the stations and sampling times were also measured (with depths ranging from 1 to 11 m). Similar but muted trends were seen in the bottom water as in surface water.

Total Suspended Sediments, Particulate Inorganic Matter, Particulate Organic Matter and Chlorophyll (Milroy)

At each station, duplicate 1L water samples were collected from two depth strata (Surface = 0.5 m below water surface; Bottom = 0.5 m above sediment-water interface) and filtered thru pre-weighed GF/F filters. Filters were then dried in oven and weighed (±0.1 mg precision). Data represent the mean concentration of Total Suspended Solids (TSS) in units of mg L^{-1}. TSS filters were then combusted in a furnace at 550° C for 30 minutes, allowed to cool to room temperature in a dessicant chamber, and re-weighed (±0.1 mg precision). Data represent the mean concentration of Total Fixed Solids (TFS) = Particulate Inorganic Matter (PIM) in units of mg L^{-1}. The mathematical difference between measured TSS & PIM values were then calculated. Data represent the mean concentration of Total Volatile Solids (TVS) = Particulate Organic Matter (POM) in units of mg L^{-1}, where POM = TSS – PIM.

At each station, duplicate 1L water samples were collected from two depth strata (Surface = 0.5 m below water surface; Bottom = 0.5 m above sediment-water interface) and filtered thru GF/F filters. All filters were stored in the dark @ -30°C. Chl-a extraction was conducted by placing each filter in a sealed test-tube in 3.00 mL of 90% acetone in the dark @ 4°C for 24 hrs. Extracted Chl-a was then measured via tri-chromatic spectrophotometric method with acid-correction of phaeopigments (EPA Method 446.0). Data represent the mean concentration (in units of ug L^{-1}) of in vivo Chlorophyll-a (Chl-a) as a proxy for algal biomass.

Water Isotopes (Alan Shiller)

Surface water samples were collected at 16 locations in Mississippi Sound during June – August 2019 as part of the USM Bonnet Carré Spillway response effort. Samples were filtered in the field using 0.45 µm syringe filters as described in Shiller (2003). The $\delta^{18}O$ and δD signatures of the water (on the V-SMOW scale) were determined using a Picarro L-2130 Cavity Ringdown Spectrometer as described in Sanial et al.

(2019). Additionally, the samples were analyzed for dissolved Mg as a proxy for salinity. This was needed because the sharp vertical salinity gradient in near surface waters made the readings from the salinity sonde occasionally difficult to match up with the actual water samples. The salinity and isotope data were then used to estimate the percentage contribution of various water sources (including Mississippi River water) to the samples following Sanial et al. (2019). Two cautions are advised in interpreting these results. First, once cannot parse the percent Mississippi River estimate into components derived from the Bonnet Carré Spillway versus that derived from Mississippi River Delta outflow since these components are isotopically indistinguishable. Second, the model of Sanial et al. assumes three-component mixing: Mississippi River water, "local" fresh water (e.g., derived from Pearl River or Mobile Bay), and offshore Gulf of Mexico seawater. Limited evidence suggests a possible groundwater component (both in the Sound and in Lake Pontchartrain) that may be isotopically heavier than the local rivers. This would result in our percent Mississippi River values being low, though probably the error is less than 10%.

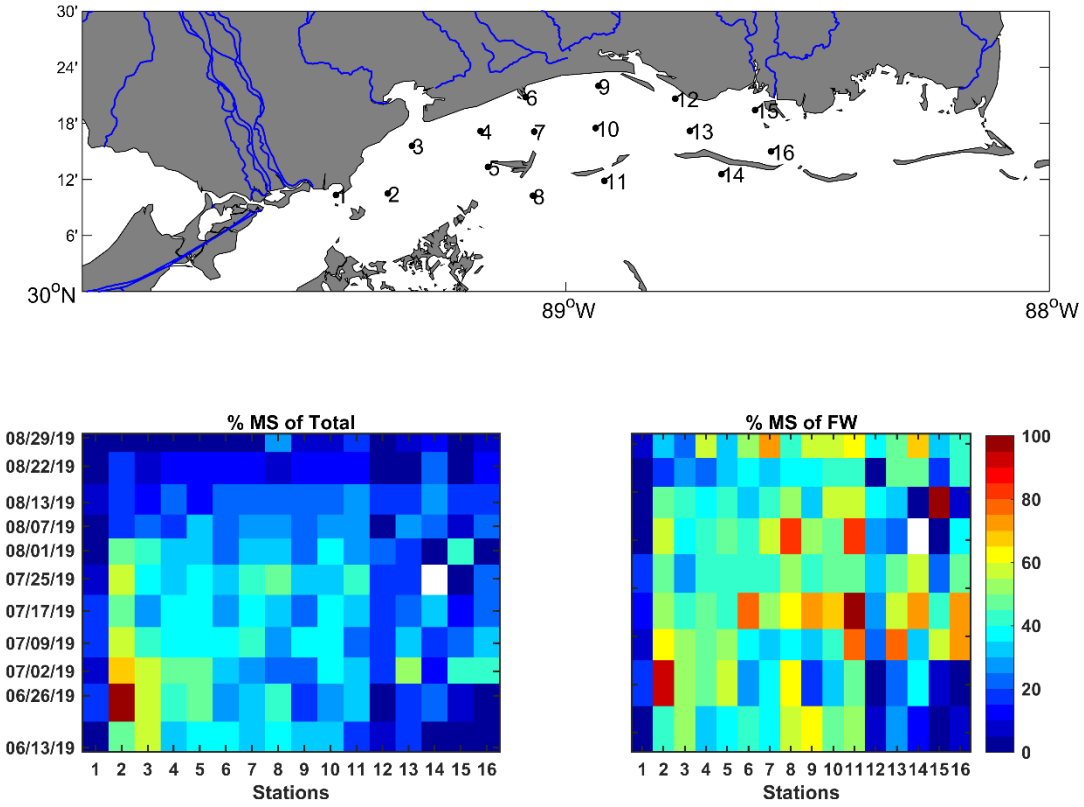

Figure 1. *(Top) Map showing survey locations in Mississippi Sound. (Bottom left) Spatial and temporal sequence showing estimate of the percentage of the sample water derived from the Mississippi River (including Bonnet Carré Spillway outflow). See color bar on extreme right. (Bottom right) Spatial and temporal sequence showing estimate of the percentage of the sample freshwater fraction derived from the Mississippi River (including Bonnet Carré Spillway outflow). See color bar on extreme right.*

Figure sequence on following pages: *Weekly spatial plots of: (Top) Salinity. (Middle) Estimate of percentage of the sample water derived from the Mississippi River (including Bonnet Carré Spillway outflow). (Bottom) Estimate of the percentage of the sample freshwater fraction derived from the Mississippi River (including Bonnet Carré Spillway outflow).*

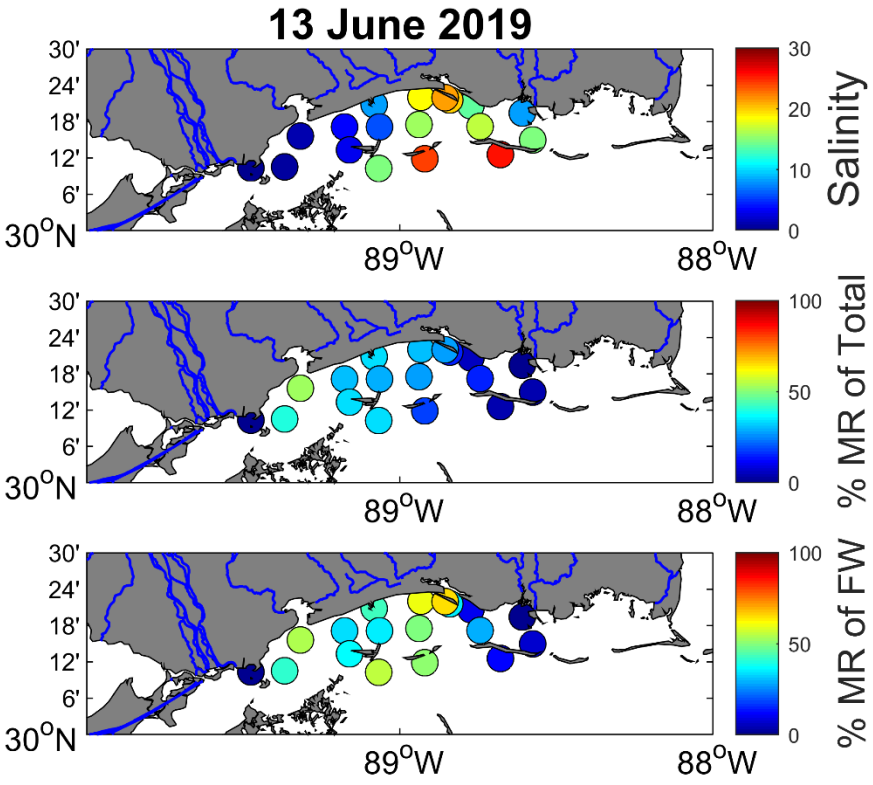
13 June 2019
30'
24'
18'
12'
6'
30°N
89°W
88°W
30
20
10
0
Salinity
100
50
0
% MR of Total
% MR of FW

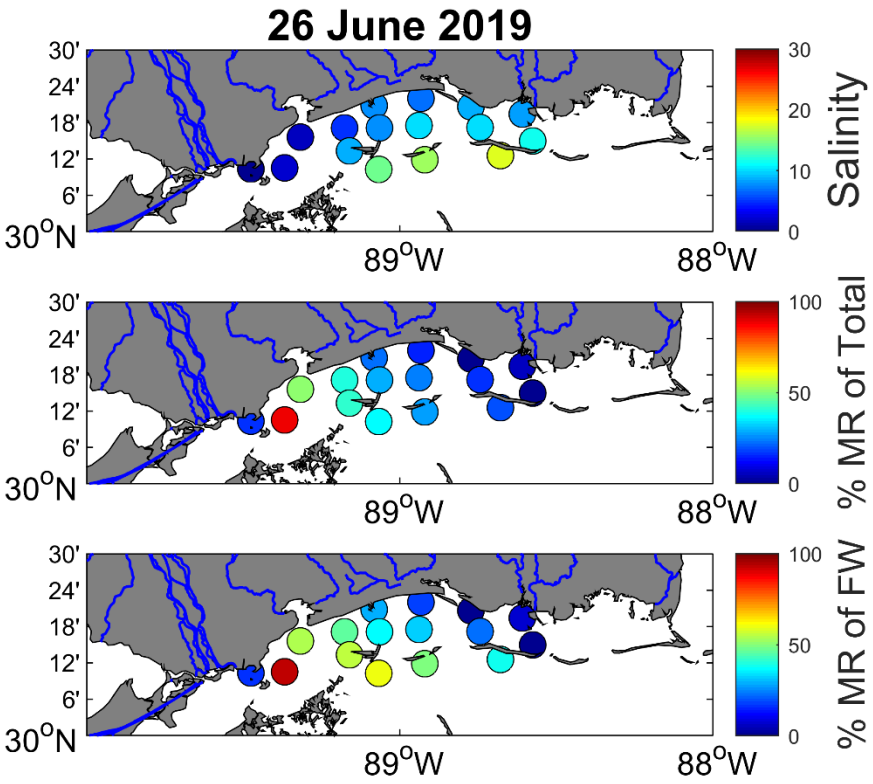
26 June 2019
30'
24'
18'
12'
6'
30°N
89°W
88°W
30
20
10
0
Salinity
100
50
0
% MR of Total
% MR of FW

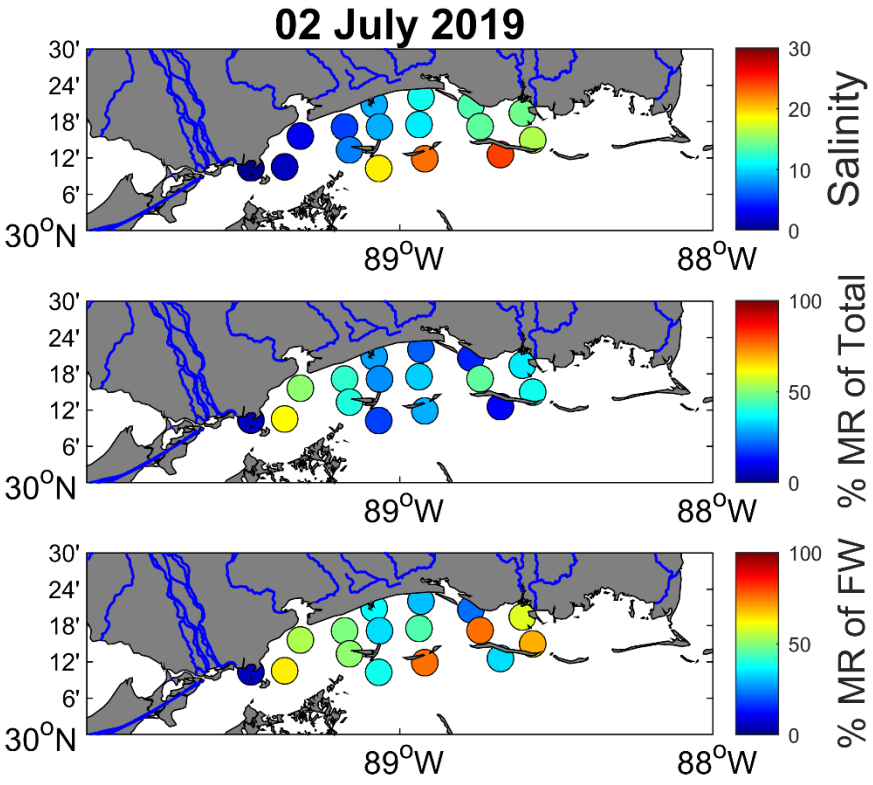
02 July 2019
30'
24'
18'
12'
6'
30°N
89°W
88°W
30
20
10
0
Salinity
100
50
0
% MR of Total
% MR of FW

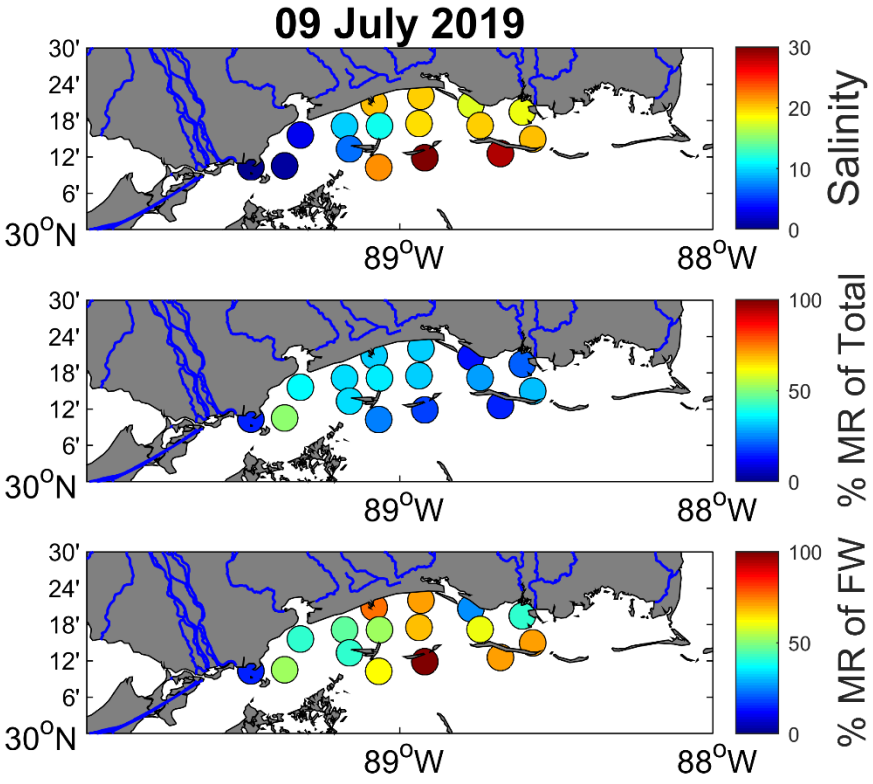
09 July 2019
30'
24'
18'
12'
6'
30°N
89°W
88°W
30
20
10
0
Salinity
100
50
0
% MR of Total
% MR of FW

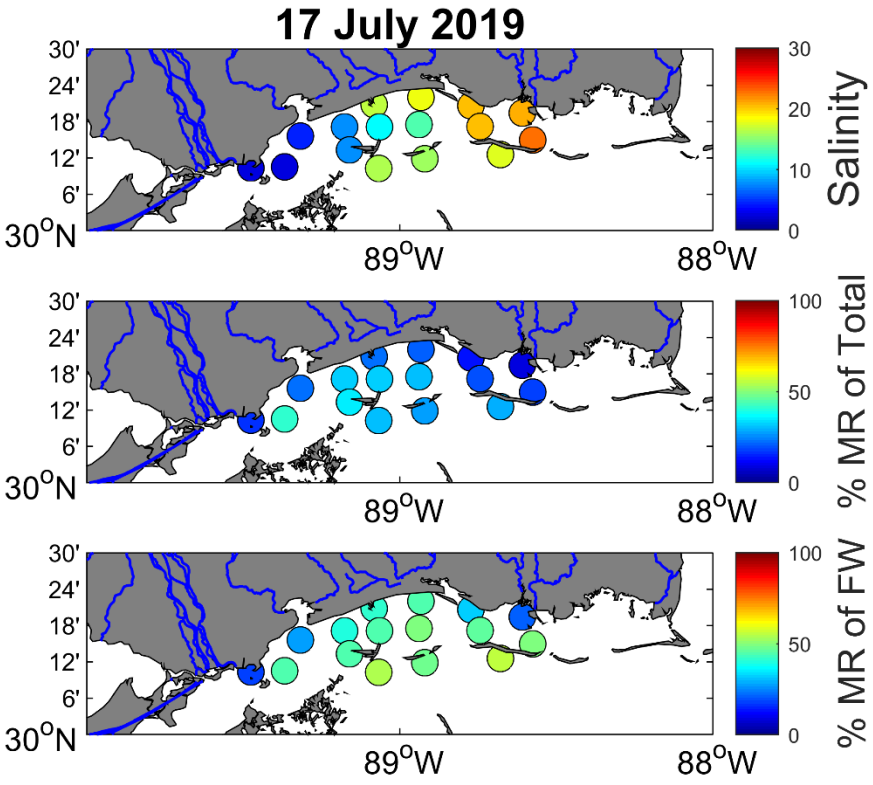
17 July 2019
30'
24'
18'
12'
6'
30°N
89°W
88°W
30
20
10
0
Salinity
100
50
0
% MR of Total
% MR of FW

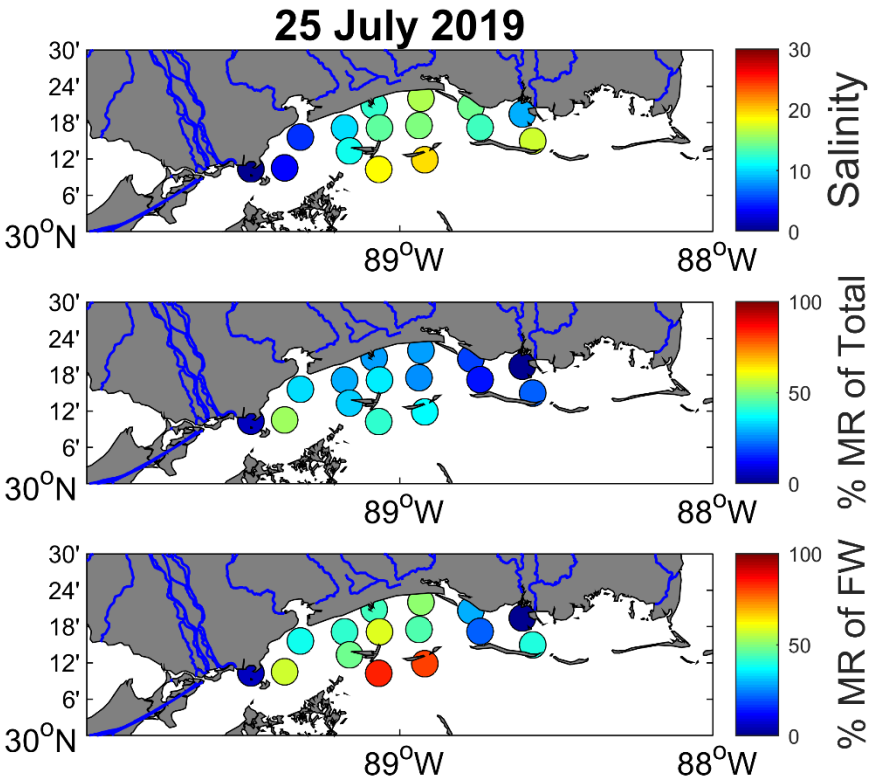
25 July 2019
30'
24'
18'
12'
6'
30°N
89°W
88°W
30
20
10
0
Salinity
100
50
0
% MR of Total
% MR of FW

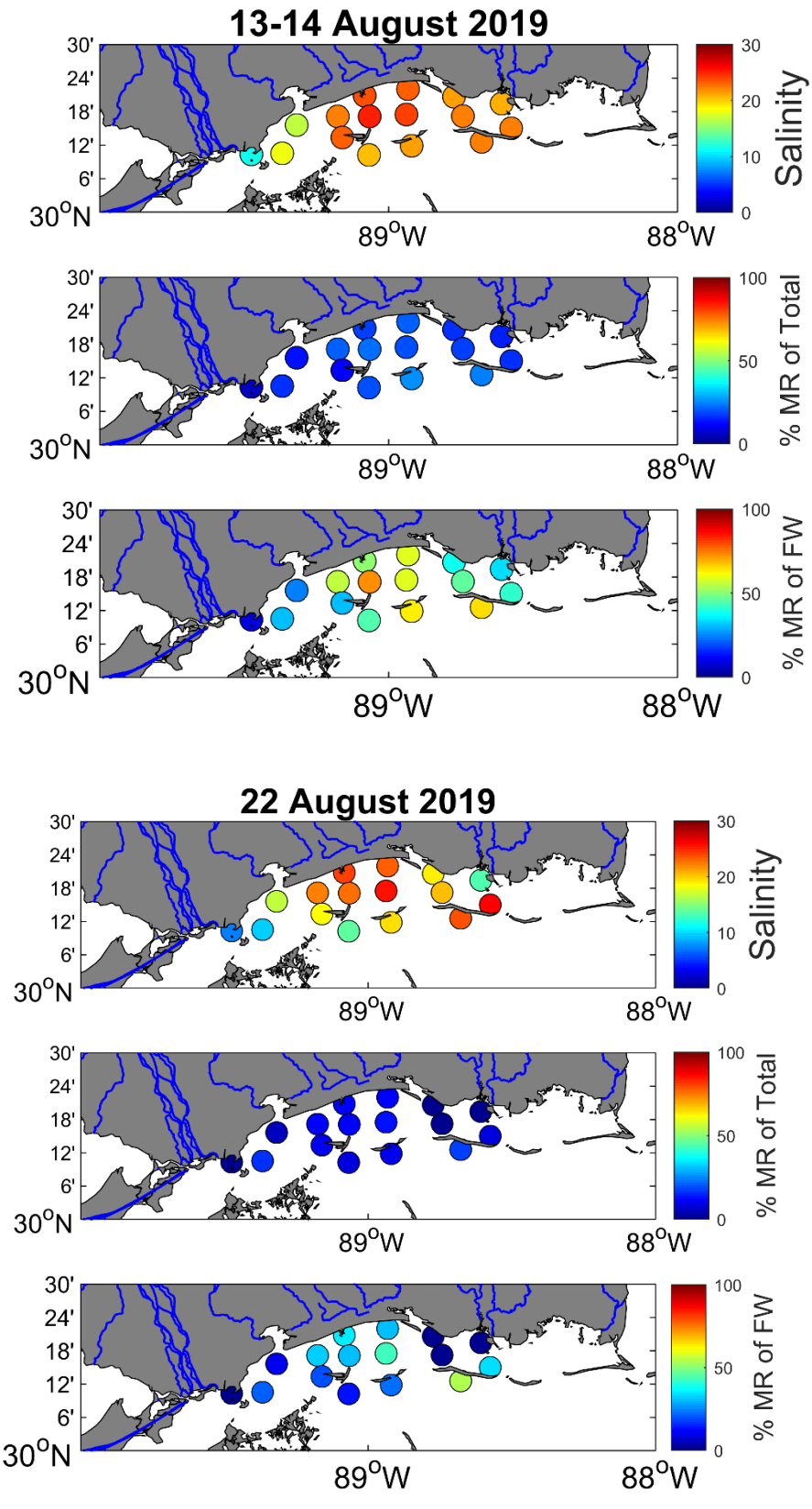
13-14 August 2019
30'
24'
18'
12'
6'
30°N
89°W
88°W
30
20
10
0
Salinity
100
50
0
% MR of Total
% MR of FW
22 August 2019

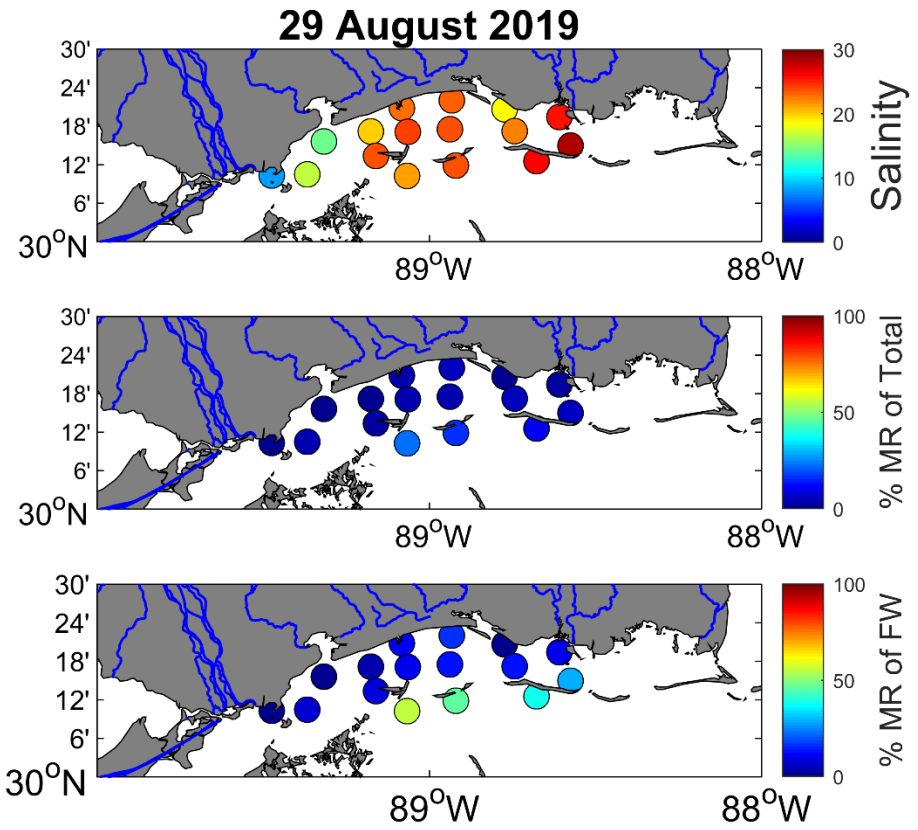

Phytoplankton Imaging Technology for Cell Identification of Mississippi Coastal Waters Impacted by Bonnet Carré Spillway (Boyette)

The primary objective was to use an advanced plankton imaging system (FlowCAM®) to provide phytoplankton cell counts and taxonomy in near real-time at selected stations located within the Mississippi Sound. The mission was to identify and count potentially harmful cyanobacteria (CyanoHAB) and other phytoplankton cells at 16 sampling stations in Mississippi coastal waters.

Date	# of Stations Sampled	Data Analyzed	Data Submitted	Report Submitted	Included in Final Report
07/09/2019	16 of 16	yes	yes	yes	yes
07/17/2019	16 of 16	yes	yes	yes	yes
07/25/2019	15 of 16	yes	yes	yes	yes
08/01/2019	16 of 16	yes	yes	no	no
08/13/2019	16 of 16	yes	yes	yes	yes
08/22/2019	16 of 16	yes	yes	yes	yes
08/29/2019	16 of 16	yes	yes	yes	yes

Microplankton (20-200 µm) community composition and cell concentration estimates (particles mL^{-1}) were conducted using a FlowCAM® Benchtop B3 Series equipped with a 532 nm green laser to detect red (> 650 nm) and orange (575 nm) fluorescence. Phytoplankton cells within a single 3.0 mL unconcentrated natural sample were imaged through a 10x objective and field of view (FOV) flow cell using trigger mode

(TM). Single aliquots of 5.0 mL per sample were run approximately > 3h after retrieval from surface stations and kept in a cooler until image analysis. Samples were manually primed via a 1.00 mL c70 syringe attached to a syringe pump with a flow rate set at 0.400 mL min^{-1}.

Post-processing consisted of examination of individual list files, which are the file extensions used by the Visual Spreadsheet software. These file types are supported only by a satellite license obtainable from Fluid Imaging Technologies, INC. Using the Visual Spreadsheet software (v. 3.7.5). Data processing included removing duplicate images and classifying each particle based on its equivalent spherical diameter (ESD), which is the diameter calculated as the mean feret measurement based on 36 sample measurements conducted at every 5^{o}. The final output for cell counts is presented in an Excel ® spreadsheet and image collages are available as portable network graphics (.png) files.

Community composition was determined manually. Cell counts for chains and colonies were not quantified. A total of 10 general phytoplankton groups were analyzed, which are determined based on water quality needs:

1. *nanoflag* is a general group of single-celled flagellates < 20µm (ESD) and includes genera within Chromophyta and Chlorophyta. **These were not quantified in this analysis.**
2. *Chlorophytes* includes freshwater and estuarine species of green algal species within Chlorophyta > 20µm (ESD).
3. *Dinoflagellates* are mixed assemblages of thecate (armored) and athecate (naked) dinoflagellates and includes HAB-forming genera.
4. *Cyano_Microcystis* includes the *Microsystis* genera of CyanoHABs.
5. *Cyano_Anabaena* includes the *Dolichospermum* (formally *Anabaena*) genera of CyanoHABs.
6. *Cyano_Other* includes mixed assemblages of cyanobacteria that do not contribute to CyanoHAB genera.
7. *Diatoms* includes all diatoms.
8. *Unidentified_filamentous* includes unidentified chains belonging to freshwater genera within Chlorophyta or Cyanophyta, which colonies present in this group may contribute to CyanoHABs (i.e. *Aphanizomenon* sp.).
9. *Microzooplankton* includes all protists that have ciliate present, including red tide-forming *Mesodinium rubrum*. This group does not produce toxins.
10. *Other* includes all other phytoplankton groups that are present (e.g. silicoflagellates, radiolarians, etc.).

CLASSIFICATION SUMMARY

07/09/2019

Overall, diatoms appear to be the predominant phytoplankton group. However, Chlorophytes, which tended to be freshwater genera (e.g. *Pediastrum, Actinastrum*, other desmids) were relatively abundant at stations in the Western Mississippi Sound, but absent in the central and eastern portion of the Sound. Dinoflagellates and nanoflagellates were abundant at all stations, but particularly at station 6, where *Scrippsiella* sp. was at elevated cell concentrations (> 250,000 cells L^{-1}). This genera is not known to produce toxins.

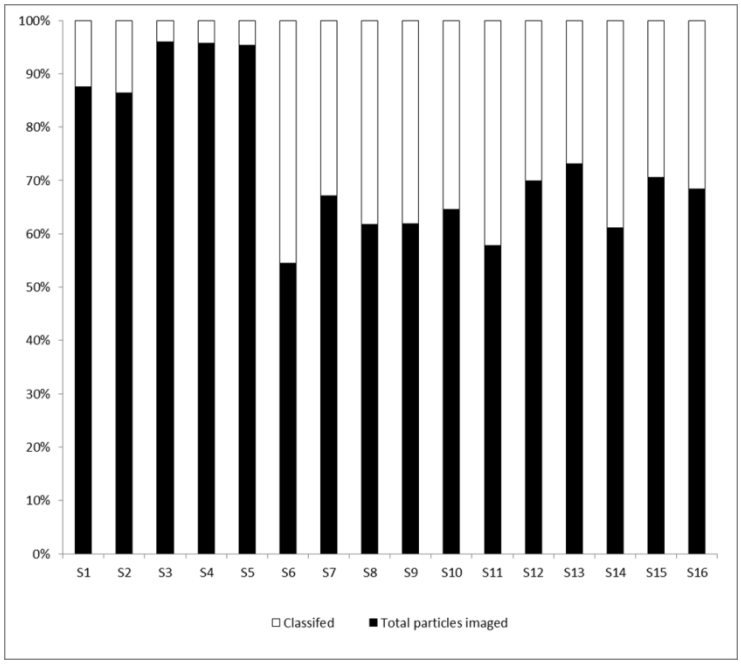

Figure 1. *Phytoplankton community classified relative to the total particles imaged.*

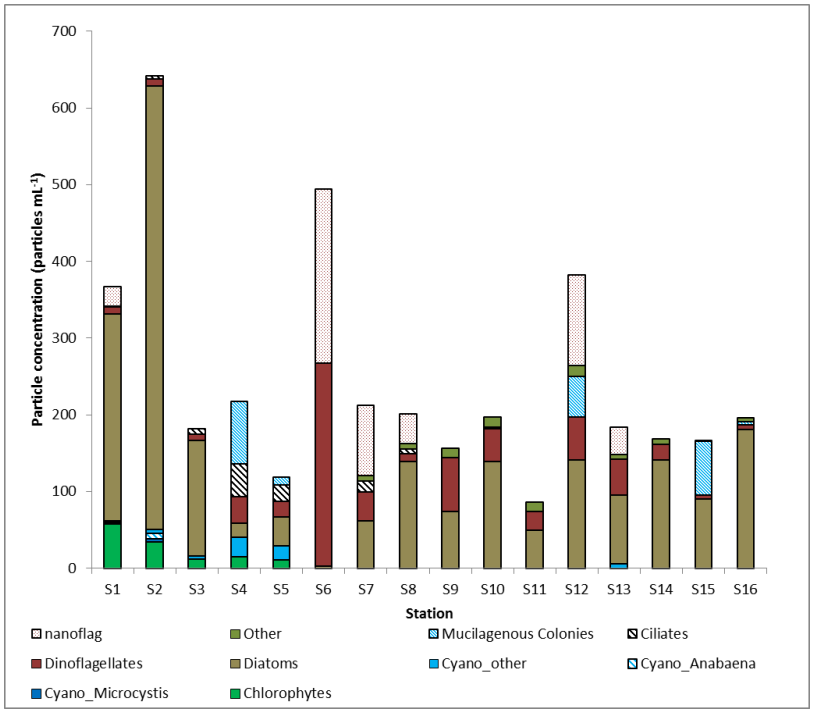

Figure 2. *Estimated particle concentration (particles mL^{-1}) for each of the 10 groups of classified images.*

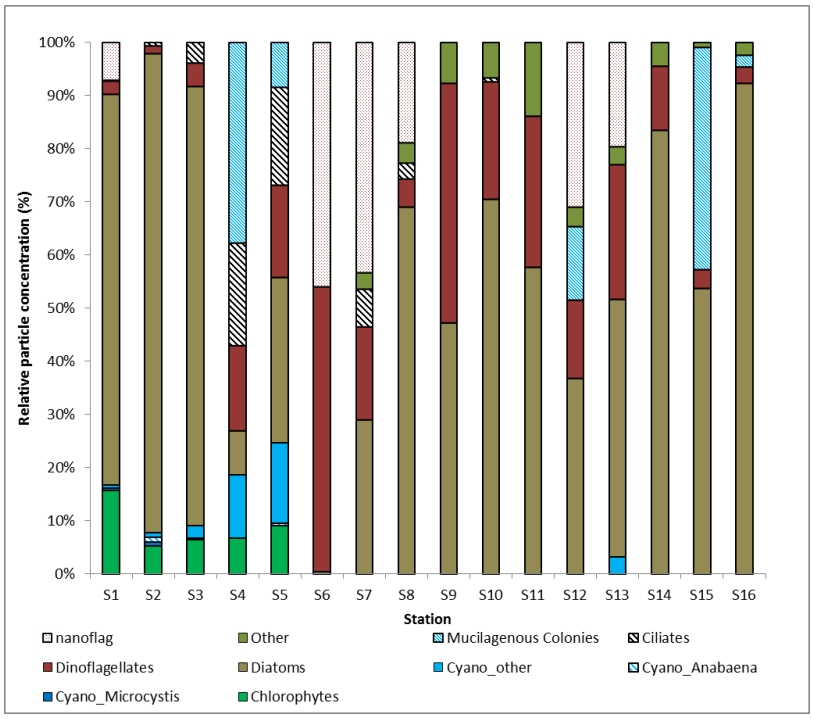

Figure 3. *Relative contribution (% frequency) of each the groups to the total classified particles.*

Cyanobacteria were present at a few stations, though the cell concentrations were significantly below "bloom" levels. *Anabaena* sp. were the most abundant at station 2, but the cell concentration estimates were significantly lower than the diatom signal (Figs. 2, 3). Station 4 presented some interesting cells (Fig. 4) that were not identifiable and were simply classified as *Mucilagenous colonies.* However, *Microcystis* sp. colonies can form similar masses. These cells need further scrutiny.

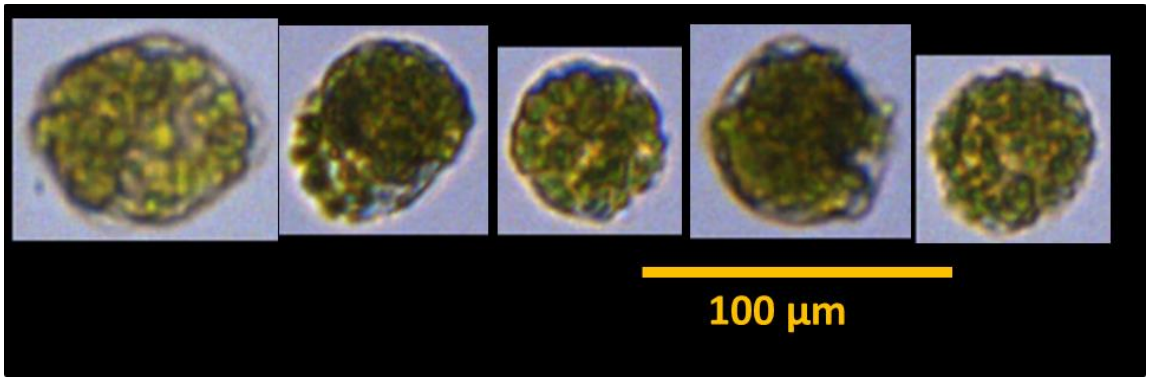

Figure 4. *Mucilaginous colonies with unidentified cells. These were later identified as* Microcystis *sp. colonies.*

07/17/2019

Total particle concentration and relative percent contribution for unclassified and classified imaged particles are presented in Fig. 5. Generally, < 30% of the imaged particles were classified. These particles were either unidentifiable detrital material or small (<15 µm) phytoplankton particles that were too small to

identify. However, these small phytoplankton particles comprise diverse groups of nanoflagellates (e.g. cryptophytes, haptophytes, and small dinoflagellates).

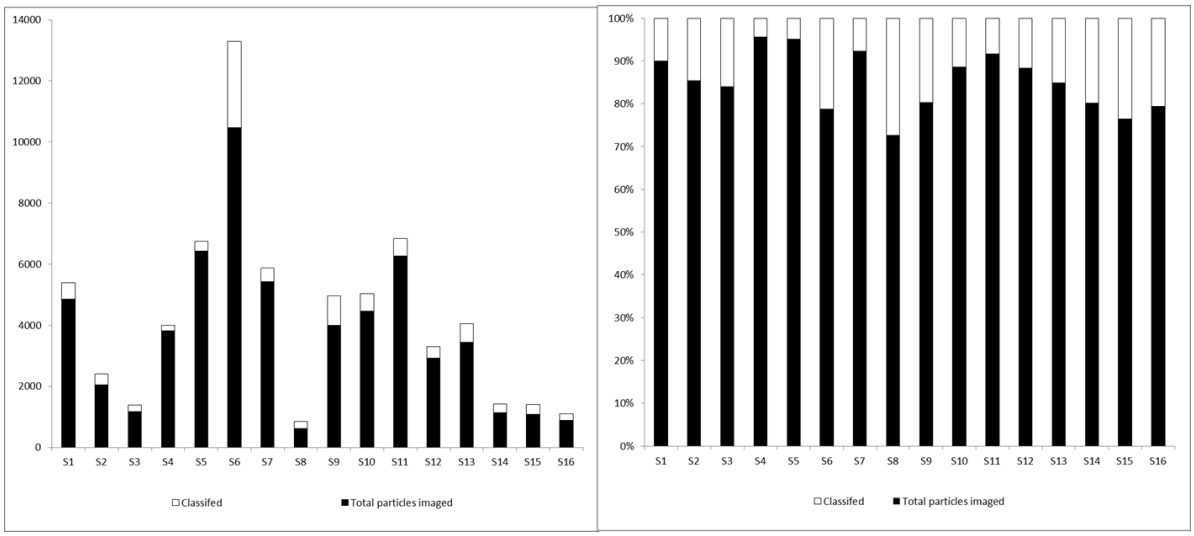

Figure 5. *Total particle concentration and relative percent contribution for unclassified (black) and classified (white) particles.*

Harmful algal bloom cyanobacteria (CyanoHABs) were present, but not at bloom concentrations in these samples (Fig. 6). *Dolichospermum* sp. were present at stations in the western Mississippi Sound, but absent at stations east of Pass Christian Harbor. Groups of cells, which were classified as *Microcystis* sp. colonies (Fig. 4.), were present in several stations in the central and eastern waters of the Mississippi Sound. Other filamentous cyanobacteria were present at stations in the eastern Sound. Several genera of fresh/brackish water chlorophytes (i.e. green algae) were present at stations throughout the study site. Diatoms were the most abundant phytoplankton community at all stations, although nanoflagellates comprised a significant portion of the classified images.

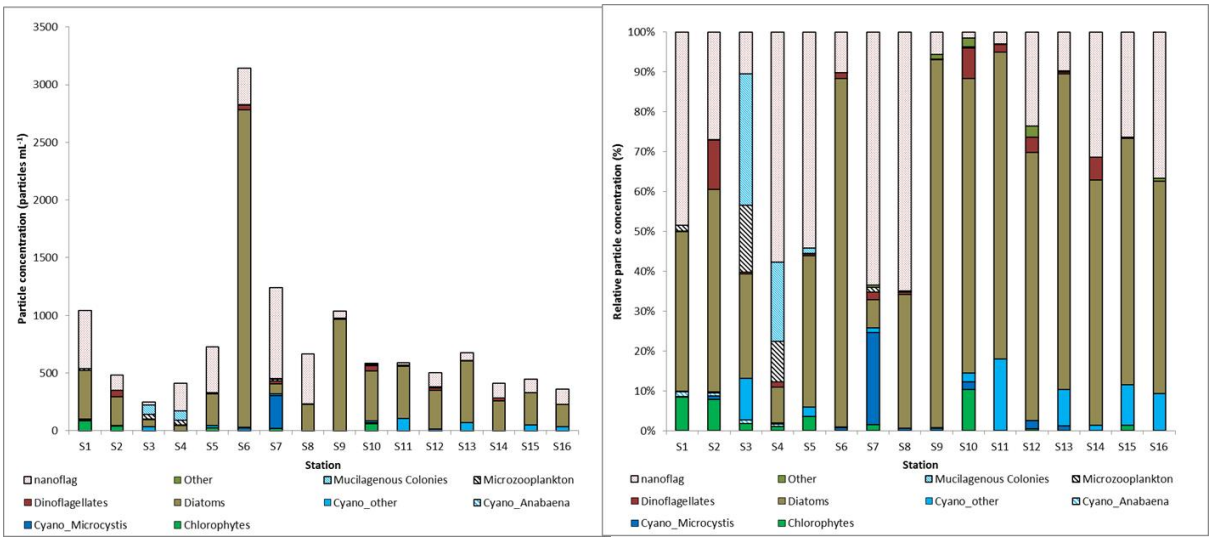

Figure 6. *Community composition of the major plankton groups during 07/17/2019 sampling.*

07/25/2019

Station S14 was not sampled due to poor ocean conditions. On average, less than 15% of the particles were classified due to their small size (Fig.1). The phytoplankton communities present in the *Unclassified < 20µm* are represented by mixed assemblages of Cryptophytes, Haptophytes, and other nanoflagellates, whereas *Unclassified > 20 µm* tends to be predominately detrital material.

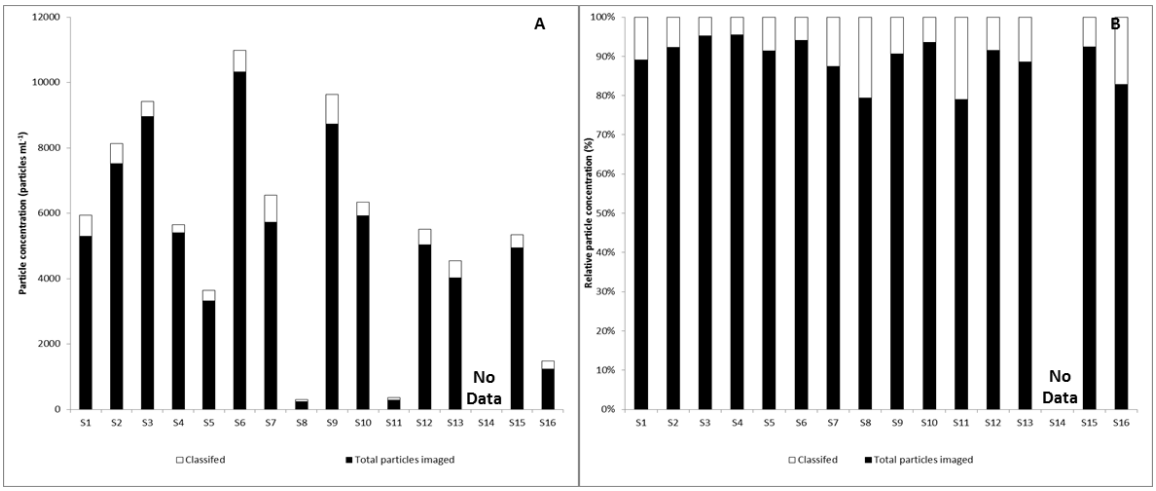

Figure 7. *Classified particle concentration (A) and relative particle concentration (%) to the total particles imaged (B).*

Overall, diatoms appear to be the predominant phytoplankton groups. However, *Microcystis* sp. colonies were prevalent at most stations, particularly at stations S06 and S13. Long filaments of freshwater chlorophytes (Fig. 8) were the most abundant (>300,000 L^{-1}) classified phytoplankton at station S01, though much less abundant at stations throughout the western and central MS Sound (Fig. 9). Additionally, smaller (<15 µm) filaments, most likely cyanobacteria, were also classified in the *Unidentified filaments* category.

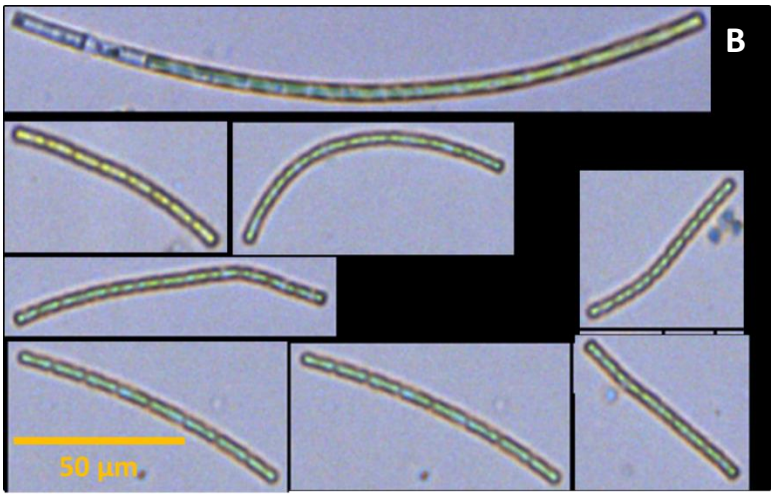

Figure 8. *Unidentified filament chains of freshwater chlorophytes.*

Other freshwater chlorophytes (e.g. *Pediastrum, Actinastrum*, other desmids) were relatively abundant at stations in the Western Mississippi Sound, but absent in the central and eastern portion of the Sound. Dinoflagellates and nanoflagellates were abundant at all stations, but particularly at stations S09, S13, and S12, where *Scrippsiella* sp., *Prorocentrum* sp. and *Ceratium* sp. were at elevated cell concentrations (> 125,000 cells L^{-1}).

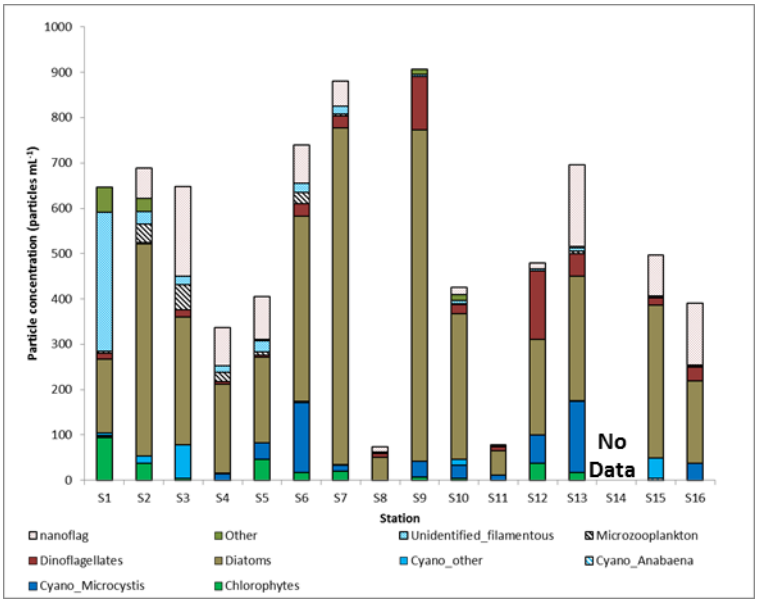

Figure 9. *Estimated particle concentration (particles mL^{-1}) for each of the 10 groups of classified images.*

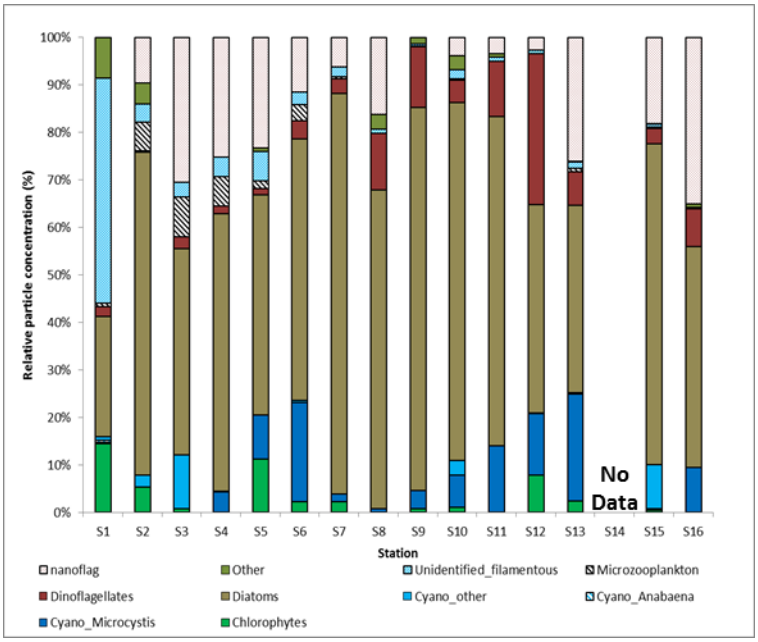

Figure 10. *Relative contribution (% frequency) of each the groups to the total classified particles.*

08/13/2019

On average, less than 15% of the particles were classified due to their small size (Fig.11) and were placed into < 20µm unclassified bins: phytoplankton communities present in the *Unclassified < 20µm* are represented by mixed assemblages of Cryptophytes, Haptophytes, and other nanoflagellates, whereas *Unclassified > 20 µm* tends to be predominately detrital material. These groups were carefully examined for any repetitive patterns of single species, indicative of a bloom. This was not found.

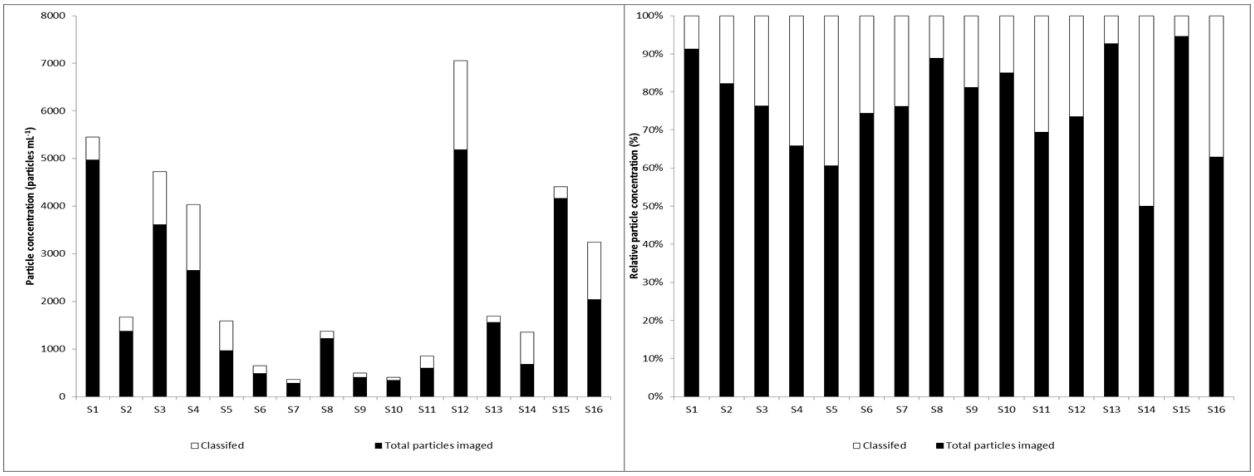

Figure 11. *Classified particle concentration (A) and relative particle concentration (%) to the total particles imaged (B).*

Overall, dinoflagellates were the predominant phytoplankton group, particularly in the eastern and western Mississippi Sound. *Microcystis* sp. colonies (Fig. 12) were present at most stations, particularly at stations S04, S05 and S16, where colonies were at elevated (>430,000 cells L^{-1}) concentrations relative other phytoplankton groups. Mixed assemblages of cyanobacteria were prevalent at S08. Long filaments of possible freshwater chlorophytes (Fig. 8), which were classified as *Unidentified filaments*, were the most abundant classified phytoplankton at station S01, though much less abundant at stations throughout the western and central MS Sound (Fig 13). Additionally, smaller (<15 µm) filaments, most likely cyanobacteria, were also classified in the *Unidentified filaments* category.

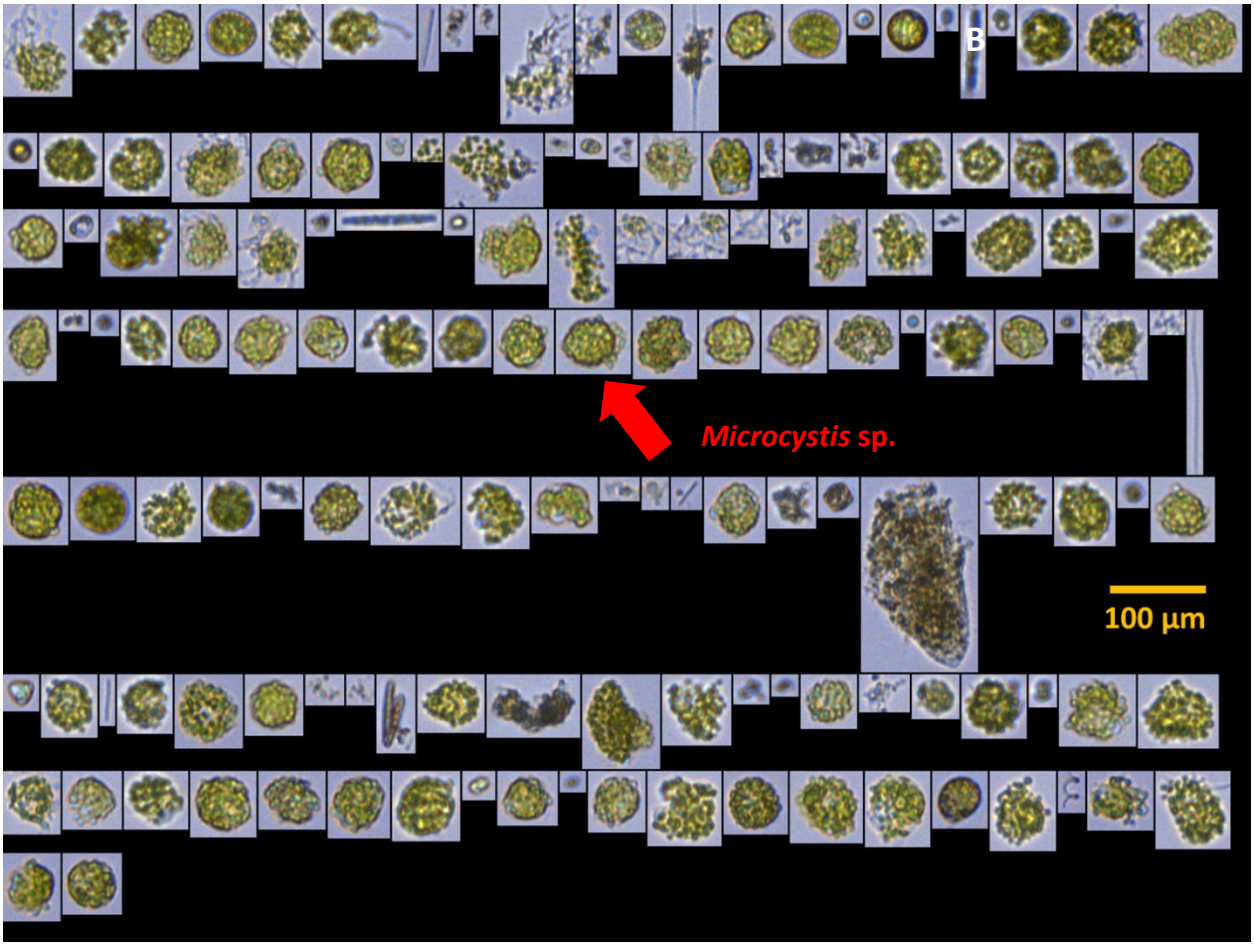

Figure 12. Microcystis *sp. colonies (red arrow pointing to example) present throughout the western and eastern MS Sound. FlowCAM Image collage of natural water sample from station S04, where colonies were at >430,000 cells* L^{-1}.

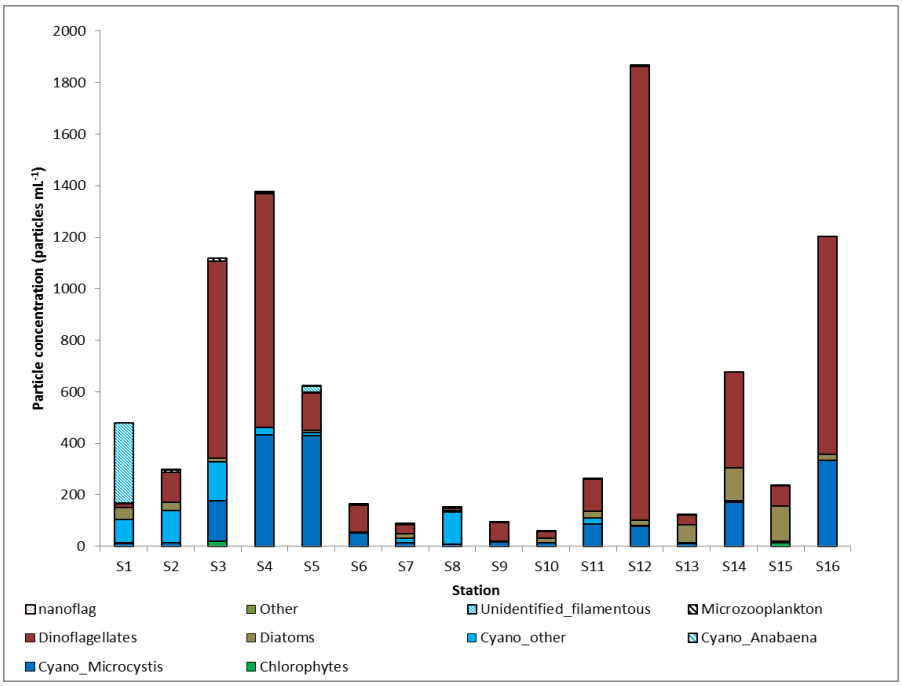

Figure 13. *Estimated particle concentration (particles mL^{-1}) for each of the 10 groups of classified images.*

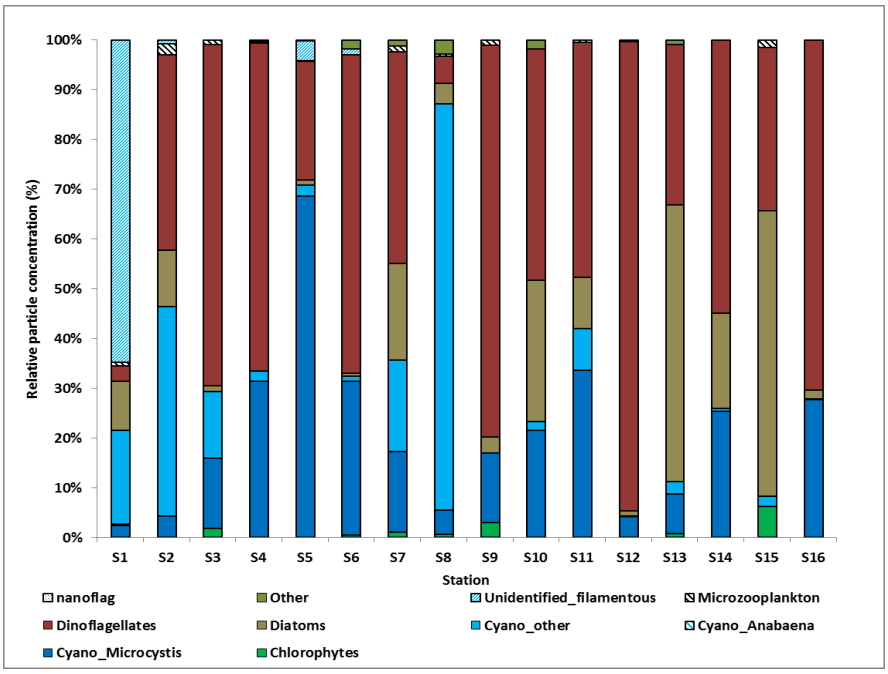

Figure 14. *Relative contribution (% frequency) of each the groups to the total classified particles.*

Other freshwater chlorophytes (e.g. *Pediastrum, Actinastrum*, other desmids) were present, but at much lower abundances than other groups. Dinoflagellates were the most abundant phytoplankton groups at all stations except stations S01, S05, and S08, where HAB-forming genera *Prorocentrum* spp., *Scrippsiella*

sp., *Dinophysis caudata* and *Ceratium* sp. were at elevated cell concentrations (> 100,000 cells L^{-1}) (Fig. 15).

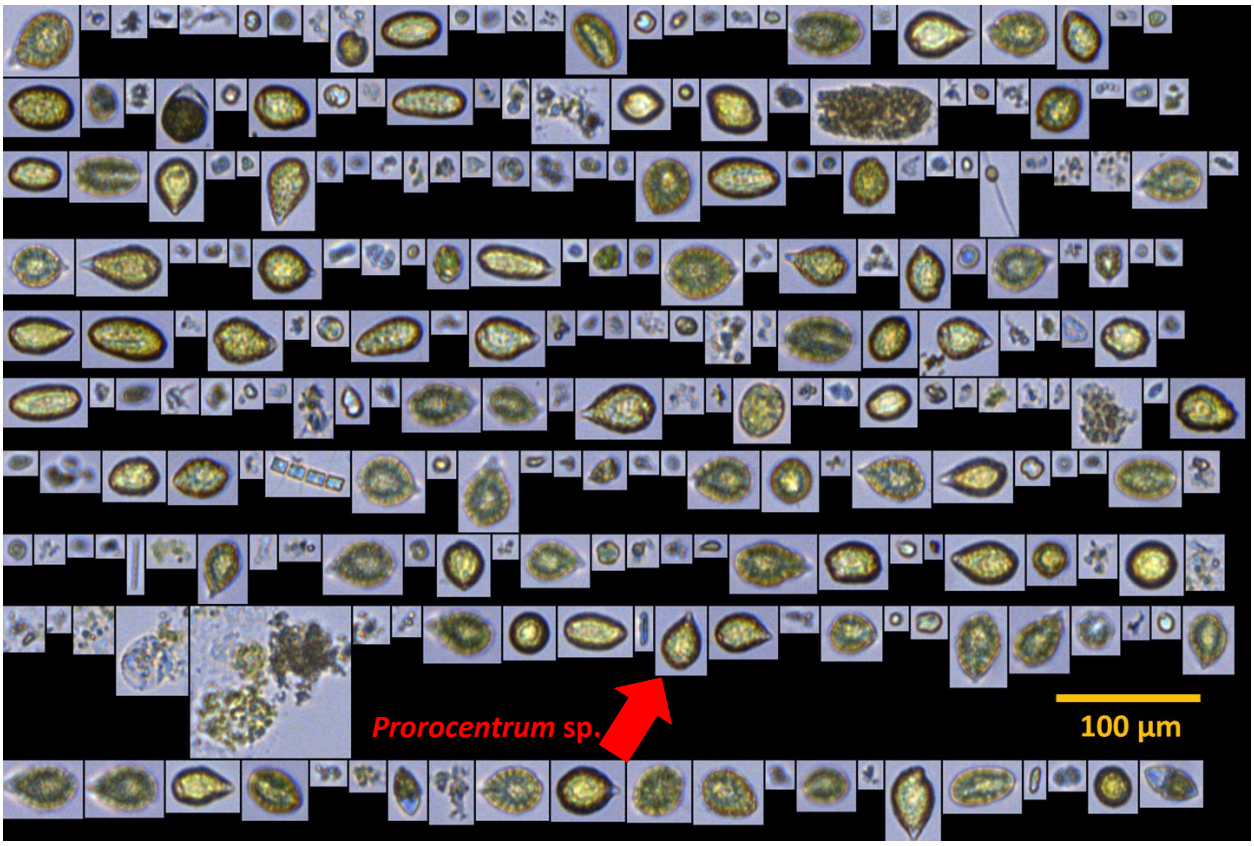

Figure 15. Prorocentrum *spp. dinoflagellates (red arrow) were the predominant phytoplankton group at stations in the western and eastern Mississippi Sound. FlowCAM Image collage of natural water sample from station S12.*

08/22/2019

On average, less than 15% of the particles were classified due to their small size (Fig.16) and were placed into < 20µm unclassified bins: phytoplankton communities present in the *Unclassified < 20µm* are represented by mixed assemblages of Cryptophytes, Haptophytes, and other nanoflagellates, whereas *Unclassified > 20 µm* tends to be predominately detrital material. These groups were carefully examined for any repetitive patterns of single species, indicative of a bloom. This was not found.

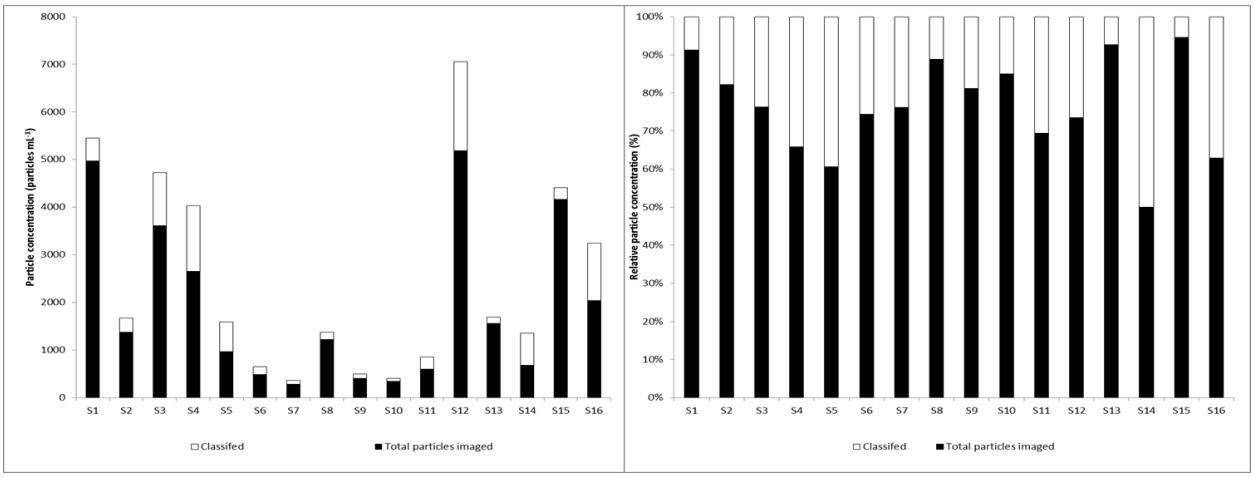

Figure 16. *Classified particle concentration (A) and relative particle concentration (%) to the total particles imaged (B).*

Overall, dinoflagellates were the predominant phytoplankton group, accounting for 48% of total classified groups. *Microcystis* sp. colonies (Fig. 17) were present at most stations (19% of the classified groups) particularly at stations S04, S05 and S16, where colonies were at elevated (>300,000 cells L^{-1}) concentrations relative other phytoplankton groups. Mixed assemblages of cyanobacteria were prevalent at S08. Long filaments of possible freshwater chlorophytes (Fig. 2B), which were classified as *Unidentified filaments*, were the most abundant classified phytoplankton at station S01, though much less abundant at stations throughout the western and central MS Sound (Fig 3). Additionally, smaller (<15 µm) filaments, most likely cyanobacteria, were also classified in the *Unidentified filaments* category.

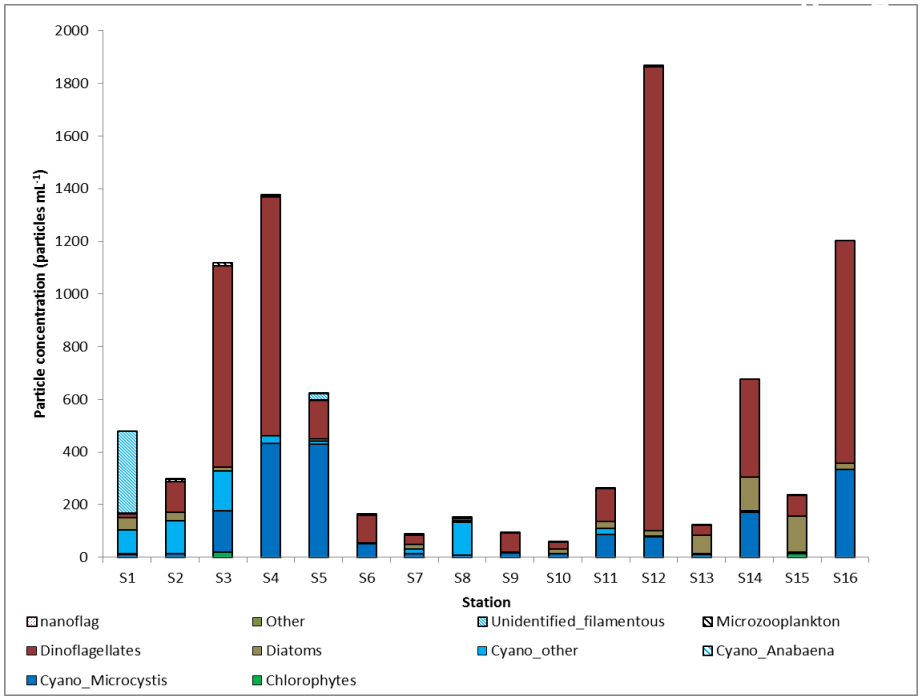

Figure 17. *Estimated particle concentration (particles mL^{-1}) for each of the 10 groups of classified images.*

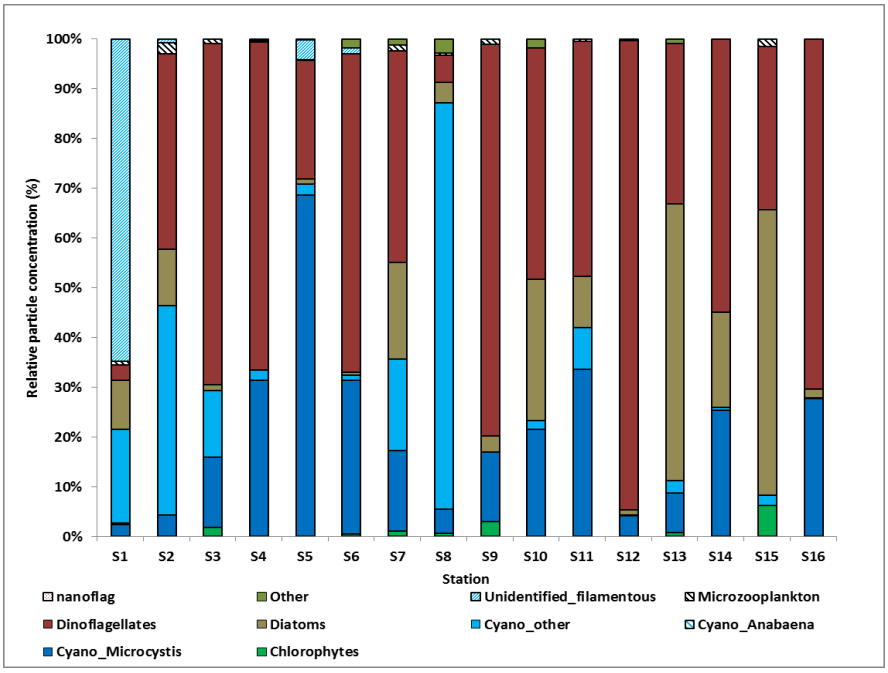

Figure 18. *Relative contribution (% frequency) of each the groups to the total classified particles.*

Other freshwater chlorophytes (e.g. *Pediastrum, Actinastrum*, other desmids) were present, but at much lower abundances than other groups. Dinoflagellates were the most abundant phytoplankton groups at all stations and especially at stations S01, S05, and S08, where HAB-forming genera *Prorocentrum* spp. were at near-bloom level cell concentrations (> 1,700,000 cells L^{-1}) (Fig. 5) and is not uncommon for this region during warm, stratified conditions in summertime.

08/28/2019

On average, less than 15% of the particles were classified due to their small size (Fig.19) and were placed into < 20µm unclassified bins: phytoplankton communities present in the *Unclassified < 20µm* are represented by mixed assemblages of Cryptophytes, Haptophytes, and other nanoflagellates, as well as small diatoms, whereas *Unclassified > 20 µm* tends to be predominately detrital material. These groups were carefully examined for any repetitive patterns of single species, indicative of a bloom. This was not found to be the case for this analysis.

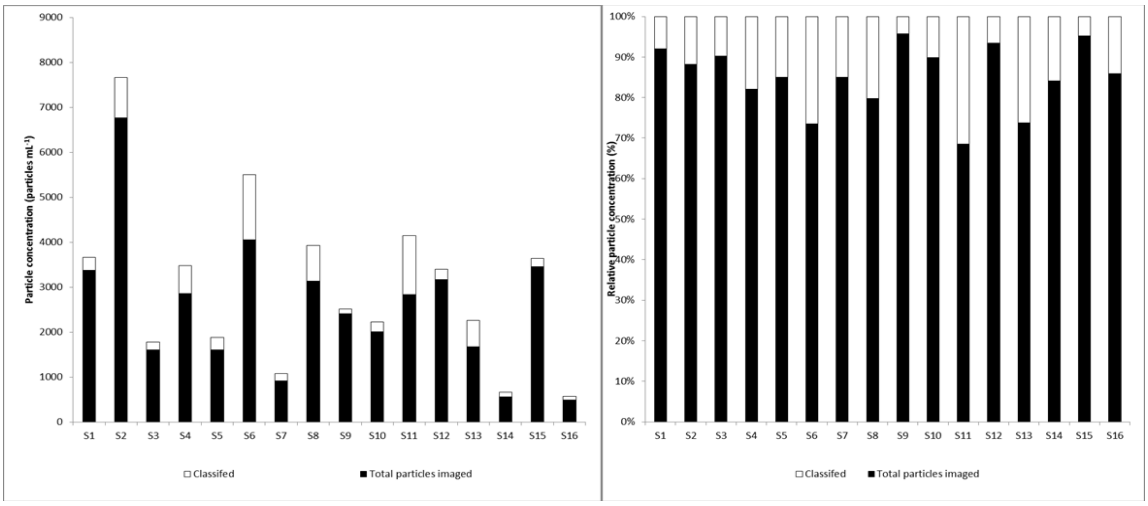

Figure 19. *Classified particle concentration (A) and relative particle concentration (%) to the total particles imaged (B).*

Overall, dinoflagellates were the predominant phytoplankton group, accounting for 39.5% of total classified groups. *Microcystis* sp. colonies (Fig. 20, 21) were present at most stations (18% of the classified groups) particularly at stations S06, S08 and S11, where colonies were at elevated (>853,000 colonies L^{-1}) concentrations relative other phytoplankton groups. Mixed assemblages of cyanobacteria were prevalent at S01 and S02.

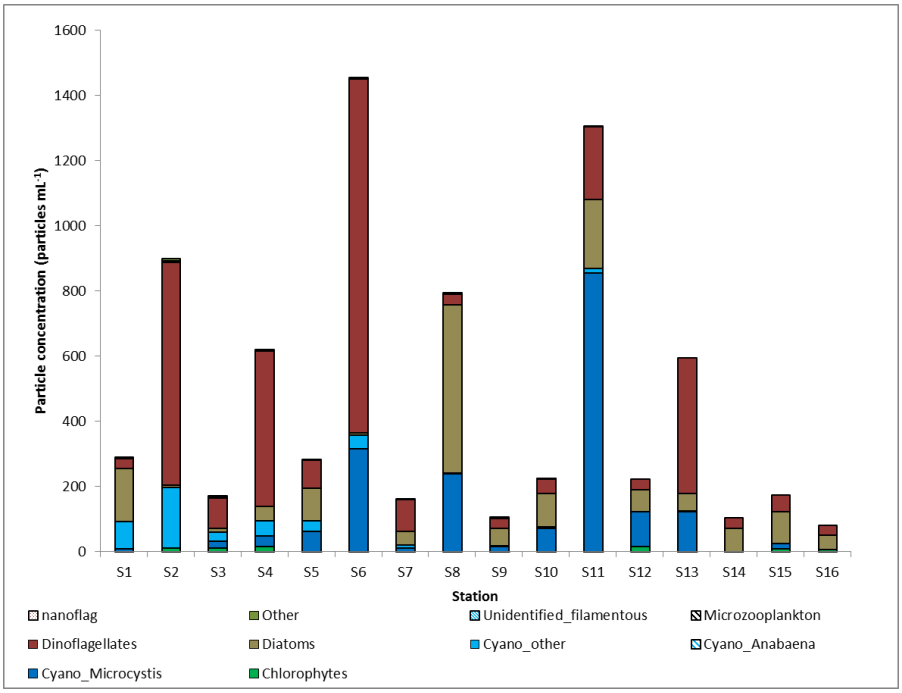

Figure 20. *Estimated particle concentration (particles mL^{-1}) for each of the 10 groups of classified images.*

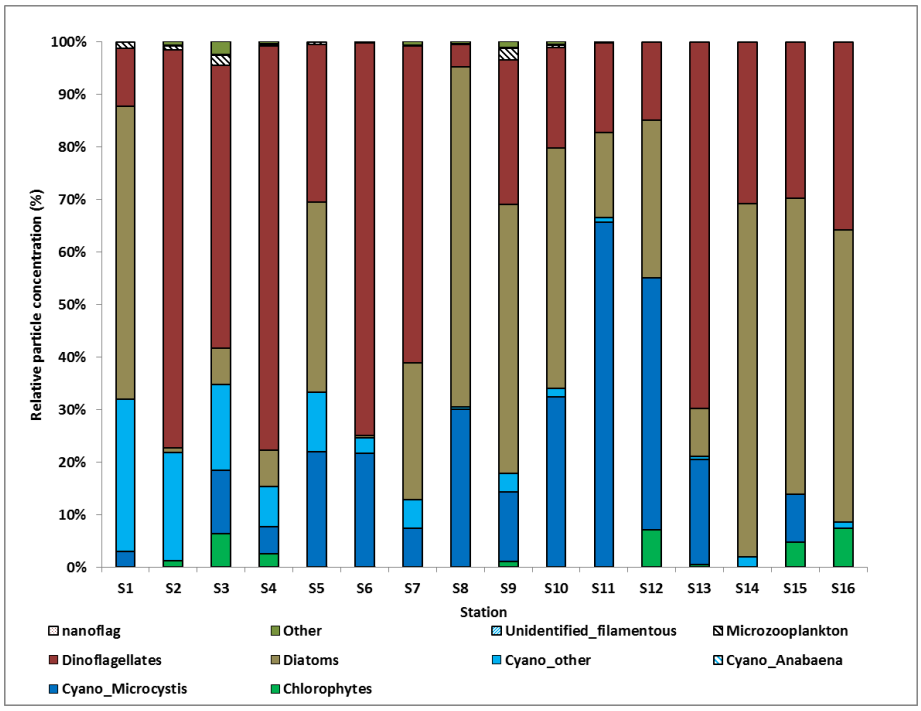

Figure 21. *Relative contribution (% frequency) of each the groups to the total classified particles.*

Freshwater chlorophytes (e.g. *Pediastrum, Actinastrum*, other desmids) were mostly absent, though there were some cells observed in the <*20µm Unclassified* category. Dinoflagellates were the most abundant phytoplankton groups at all stations and especially at stations S02, S04, S06, and S13, where HAB-forming genera *Prorocentrum* spp. were at near-bloom level cell concentrations (> 1,000,000 cells L^{-1}) (Fig. 20) and is not uncommon for this region during warm, stratified conditions in summertime.

Inorganic and Organic Nutrients and Dissolved Organic Carbon (Dillon)

Water samples at each station were collected from surface (0.5m below surface) and bottom (0.5 m from bottom) waters with niskin bottles and then stored in 1L acid washed Nalgene bottles after three rinses with sample water. Bottles were kept on ice and returned to the laboratory where water samples were filtered through muffled (500º C for 2 hours) Whatman GF/F filters using acid washed glass syringes and a clean stainless steel inline filter holder. Nutrient samples were filtered into acid washed and sample rinsed 60 ml Nalgene bottles and DOC/DON samples were filtered into muffled (500º C for 4 hours) 22 ml glass vials with Teflon lined septa caps. All water samples were frozen immediately after filtration and stored at -20º C until analysis.

Prior to analysis all water samples were slowly thawed at room temperature. All water samples were analyzed for concentrations of soluble reactive phosphate (PO_4), ammonium (NH_4), nitrite (NO_2), nitrate (NO_3), dissolve organic carbon (DOC) and dissolved organic nitrogen (DON). NH_4 concentrations were measured colorimetrically (Bower and Holm-Hansen, 1980) as were NO_2 and PO_4 (Strickland and Parsons, 1972). NO_3^- + NO_2^- was measured with a Model 42i Thermo Scientific chemiluminescent NO_x analyzer (Bramen and Hendrix, 1989). NO_3^- concentrations were then determined as the difference between NO_3^- + NO_2^- and NO_2^-. Dissolved organic carbon (DOC) and total dissolved nitrogen (TDN) concentrations were

analyzed with a Shimadzu TOC-V analyzer equipped with a Shimadzu TNM-1 total nitrogen chemiluminescent detector. DON concentrations were calculated as the difference in TDN and DIN concentrations: [DON] = [TDN] – [DIN], where [DIN] = $[NH_4^+]$ + $[NO_2^-]$ + $[NO_3^-]$.

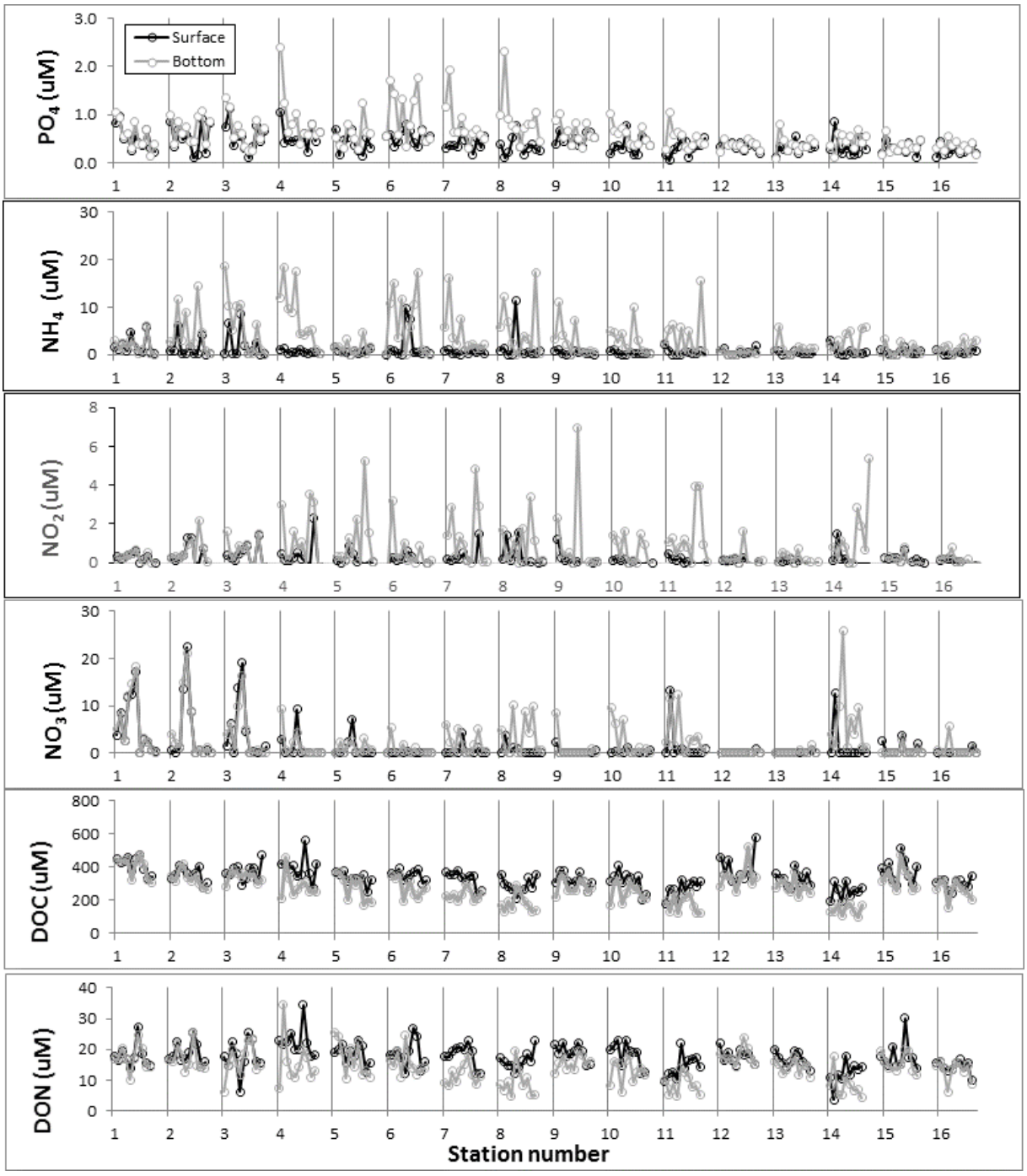

Figure 1. *Soluble reactive phosphate (PO_4), ammonium (NH_4), nitrite (NO_2), nitrate (NO_3), dissolved organic carbon (DOC) and dissolved organic nitrogen (DON) concentrations at each sampling site over 11 sampling events from June to August 2019. Each numbered panel section contains a station's time series for each parameter measured.*

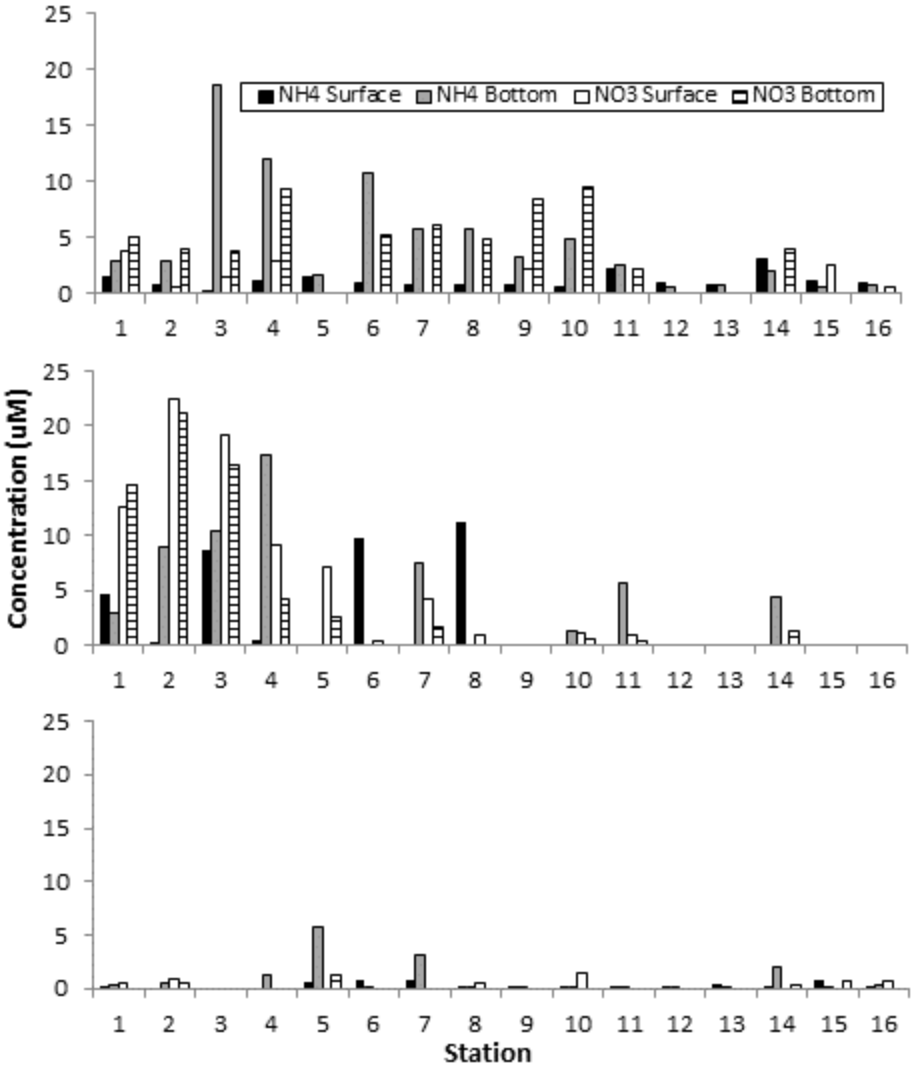

Figure 2. *Surface and bottom water ammonium and nitrate concentrations at all stations on June 13 (top panel), July 17 (middle panel) and August 29, 2019 (bottom panel).*

USGS/MSDMR Gauge Data for Mississippi Sound (Stephan Howden)

The hydrological monitoring stations in the Mississippi Sound, operated in partnership between the United States Geological Survey (USGS) and the Mississippi Department of Marine Resources (MDMR) and the NOAA meteorological station at the Bay Waveland Yacht were analyzed for the majority of the period of time that the Bonnet Carré Spillway (BCS) was opened in 2019. Figure 1 compares the time series of BCS discharge to the annual freshwater input into the Mississippi Sound and outflow from Mobile Bay. Figure 2 is a copy of the map of the USGS/MDMR real-time water quality stations from the website https://dmr.ms.gov/wp-content/uploads/2019/09/Interactive-USGS-Map.pdf.

Figure 1. *Freshwater input into the Mississippi Sound. Left: BCS discharge during each opening till late July, 2019 compared with annual average discharges into the Mississippi Sound and from Mobile Bay. Middle: locations of rivers from Table at right. Right: Annual average freshwater discharges compiled from USGS.*

Table 1 lists information about the western most USGS/MDMR hydrological monitoring stations. Figures 3 and 4 show the long-term salinity time series from the stations in Table 1. It is evident that the low salinity event associated with the 2019 BCS opening is unprecedented in the approximately 10 year record. It is important to point out that these stations have instruments moored at about 1 m from the seafloor (MDMR, personal communication) and may be saltier than surface waters.

Figure 5 illustrates the relationship between wind direction and salinity in the western Mississippi Sound. Wind data are from the NOAA weather station located at the Bay Waveland Yacht Club, and are 48 hour low-pass filtered. There is a clear relationship between wind directions and salinity in the 3 westernmost stations, with high salinities when winds are blowing from the east-northeast and low salinities when winds are blowing from the south-southwest. This is an important result because summer is when winds mostly come from the south-southwest and this would be a time to avoid freshwater discharges for coastal restoration east of the Mississippi River delta.

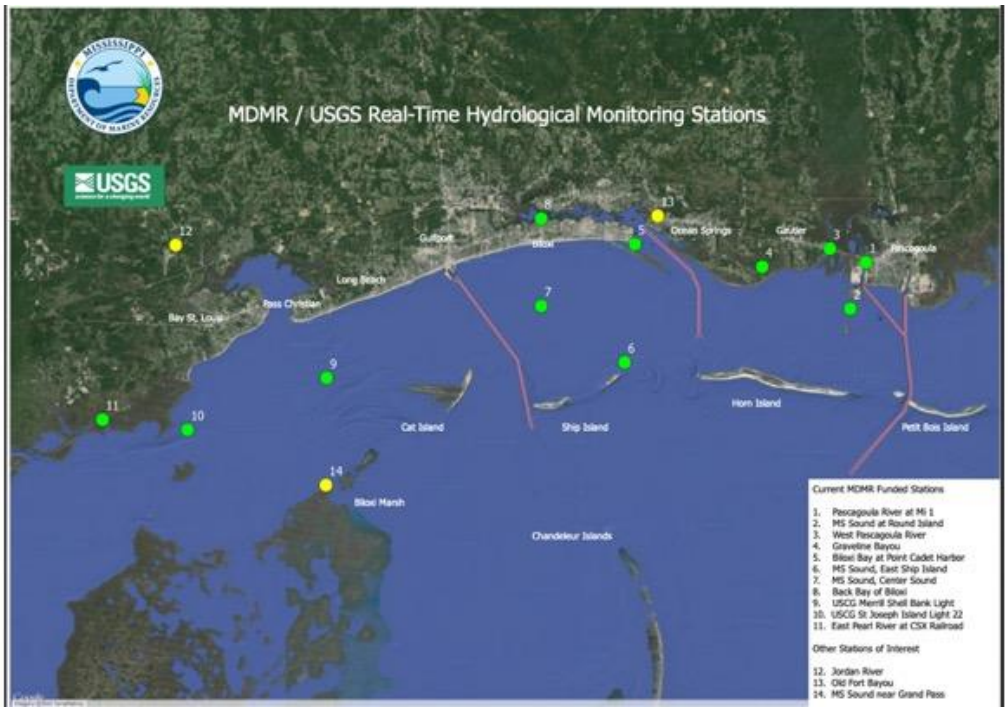

Figure 2. *Map of USGS/MDMR real-time water quality stations.*

Table 1. *Information on USGS/MDMR water quality stations in the western Mississippi Sound.*

MSDMR Station #	Name	USGS Station Number	URL	Lat	Lon	Begin Data	End Data		Headerlines
10	TJOSEPH ISLAND LIGHT	301104089253400	https://nwis.waterdata.usgs.gov/nwis/inventory/?site_no=301104089253400&agency_cd=USGS	30°11'27"	89°25'20"	2008-12-17	present	H,T,Sc,S	33
9	MERRILL SHELL BANK LIGHT	301429089145600	https://waterdata.usgs.gov/nwis/uv?site_no=301429089145600	30°14'17"	89°14'34" NAD27	2008-12-03	present	H,T,Sc,S	33
14	Mississippi Sound near Grand Pass	300722089150100	https://waterdata.usgs.gov/nwis/uv?site_no=300722089150100	30°07'22"	89°15'01"	2008-10-01	present	Wdir, Wspd, T,Sc,H,S	36
6	EAST SHIP ISLAND LIGHT	301527088521500	https://waterdata.usgs.gov/nwis/uv?site_no=301527088521500	30°15'16"	88°52'08"	2008-08-29	Present	T, Sc, H, Turb, DO, S	36
7	GULFPORT LIGHT	301912088583300	https://waterdata.usgs.gov/nwis/inventory/?site_no=301912088583300&agency_cd=USGS	30°19'07"	88°58'20"	2009-01-22	Present	H,T,Sc,S,Turb,DO	35

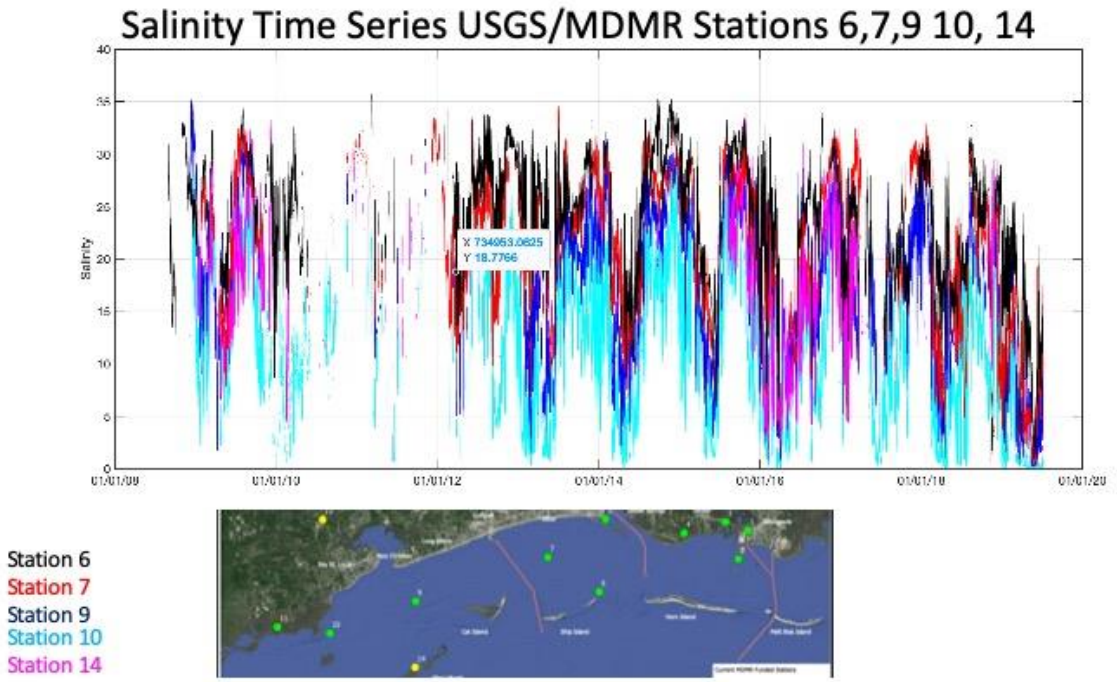

Figure 3. *Long-term salinity time series at stations 6, 7, 9, 10 and 14.*

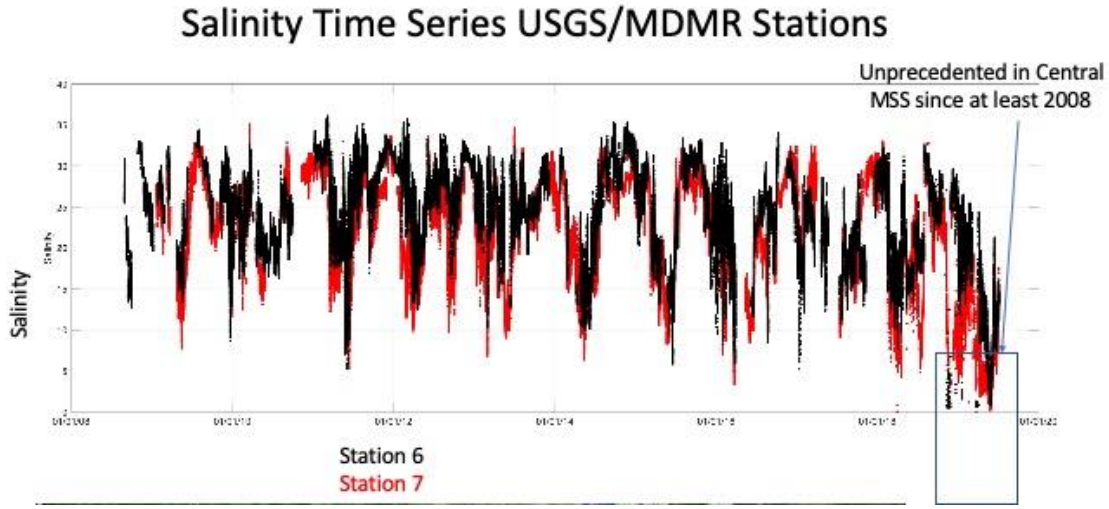

Figure 4. *Long-term salinity time series at stations 6 and 7 showing unprecedented low salinity event.*

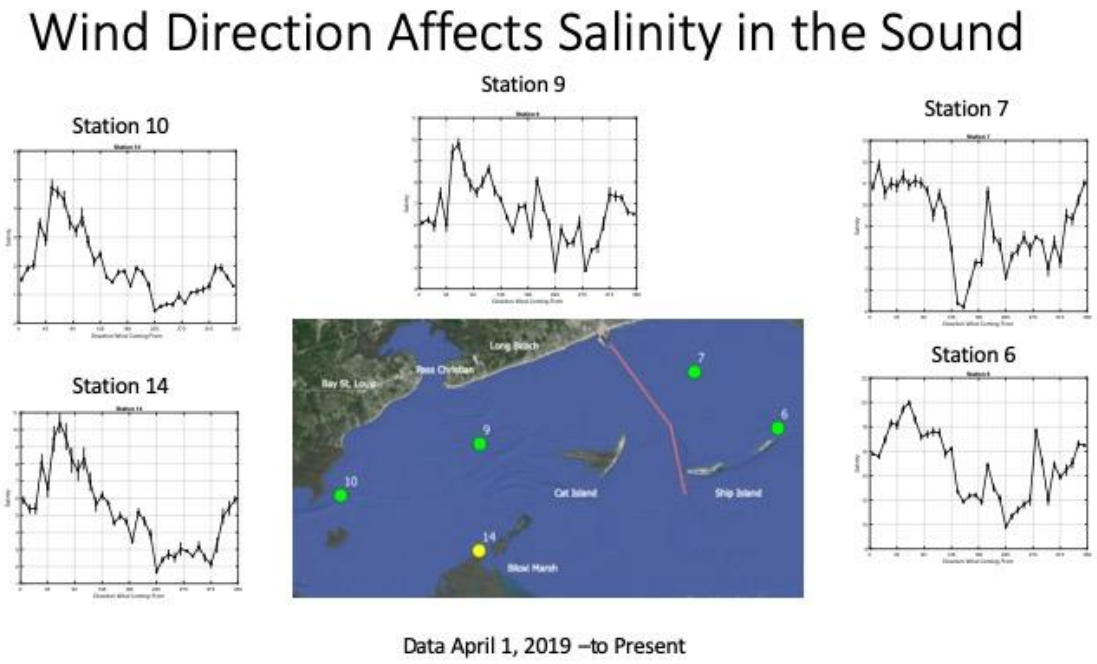

Figure 5. *During BCS event 48 hour low-pass filtered wind-direction correlated with salinity, especially with western-most stations. High salinities when winds are coming from the north east to east, and lowest salinities when winds coming from the south-southwest for the three western-most stations.*

Component 2: Remote Sensing and Circulation Modeling

Component Lead Investigator: Kemal Cambazoglu
Co-PIs: Jerry Wiggert, Diana Bernstein

It is critical to understand the circulation and transport of the water from the Bonnet Carré Spillway (BCS) opening events when significant volumes of freshwater enter the estuarine waters of the Mississippi Sound. The remote sensing and modeling group provided satellite ocean color data, ocean modeling data and atmospheric modeling data during the project. These satellite data and model forecast data provided the broader project team with current and projected conditions across the study area before, during and after field sampling efforts and also provided an overview of the spatial and temporal variability of freshwater influence.

Methods

Satellite data: Satellite data were acquired daily from NOAA's Comprehensive Large Array-Data Stewardship System (CLASS) [1]. Ocean color satellite imagery from the Visual Infrared Imaging Radiometer Suite (VIIRS) was processed to Level 3 at 750m resolution using the Naval Research Laboratory's N2gen code based on NASA's L2gen software [2] and standard atmospheric correction [3]. Contamination from land, clouds, sunglint and other disturbances to the radiance signal was masked using standard flags. Particle backscattering at 551 nm (m-1) was derived using the Quasi-Analytical Algorithm (QAA) [4,5]. Remote sensing optical backscattering indicates the presence of the freshwater plume and the associated suspended material near the surface of the water.

Ocean model data: The modeling group acquired and processed Northern Gulf of Mexico Operational Forecast System (NGOFS) data for the Mississippi Sound and Bight. Surface salinity and surface current results from the model were provided daily. NGOFS is based on a three-dimensional, high resolution unstructured grid model, Finite Volume Community Ocean Model (FVCOM) [6]. The grid resolution ranges from 10 km in the open ocean to approximately 600m near the coast and down to 200-300 m along navigational channels. Hourly NGOFS output was acquired from NOAA's Center for Operational Oceanographic Products and Services server (CO-OPS) [7,8].

Atmospheric model data: The Weather Research and Forecasting Model (WRF) [9] was used to create hourly wind field products. The output from a 3-km resolution of the High Resolution Rapid Refresh (HRRR) model [10] for the domain over the contiguous United States was acquired from the cloud storage system at the University of Utah [11]. The native model output for surface wind speed and direction was interpolated on a 1-km grid over the Mississippi Sound. For the water sampling field campaign purposes, we produced wind field forecasts 24 hours before each sampling. For the forecast, HRRR output data was downloaded from the National Oceanic & Atmospheric Administration website [12].

Results

Modeling group have provided the entire project team with the images for satellite ocean color data, ocean model forecast data and atmospheric model forecast data in a folder created on a USM server.
Daily satellite images for February 2019 to August 2019 covering both openings of the spillway in 2019 were produced. Satellite ocean color data included particulate backscattering coefficient (bb551) for all months and also included chlorophyll-a (chla) on an as-needed basis for the second opening time period of the spillway (June-to-August).

Particulate backscattering satellite imagery shows the distribution of river-borne sediments at the surface of coastal waters. Warmer colors (yellow to red) in the western Mississippi Sound indicated the extent of freshwater influence from diverted river water from the Bonnet Carre Spillway discharge. Deep red colors

are representative of salinities less than 5 ppt, and blue colors represent high salinity waters. Figure 1 shows particulate backscattering coefficient (bb551) derived from satellite ocean color data over the study area in May 2018 in panels (a), (c), (e) when there was no spillway opening versus May 2019 in panels (b), (d), (f) when the spillway was open from February 27 to April 11 2019 and was re-opened on May 10, 2019. It may be seen that there already was more particulate material in the system before the second opening. Figure 2 (a) thru (k) shows particulate backscattering coefficient (bb551) derived from satellite ocean color data over the study area after the 2nd spillway opening in 2019. The shallow estuarine system is heavily influenced by winds and satellite imagery supported field observations of reduced spillway-related freshwater effects in the central Sound in association with winds. Chlorophyll-a images were generated and analyzed to assist with the detection of potential harmful algal bloom locations to assist MDMR. Figure 3 shows an example from June 2019 with very high chl-a regions. While chl-a imagery is not sufficient to serve as a proxy for HABs, very high chl-a may be indicative of which areas to focus on as potential HAB locations and may assist with adaptive sampling efforts.

Wind speed and direction fields from the WRF atmospheric model were produced for May 2019 to August 2019. The surface wind fields were created hourly for each day and plotted out at 6:00 PM local time, which is around the daily overpass of the satellite. Hourly forecast winds were created weekly ahead of those days with a field sampling campaign. Figure 4 presents an example of the dynamic nature of wind variability in the study area and how winds can dramatically change within hours due to fronts passing over the study area and due to sea-land breeze circulation.

Hourly surface salinity and current forecast fields from NGOFS ocean modeling system were produced for those days of field sampling campaigns. Figure 5 shows surface salinity and currents forecast fields created using NGOFS output. These images were produced hourly and provided to the scientific team before weekly field sampling campaigns in July 2019.

Both atmospheric and ocean modeling products provided an overview of conditions ahead of measurement activities in the field. The project team created animations of hourly wind products as well as hourly surface salinity and current products so that the spatio-temporal variability and changes in winds, circulation and the surface water response may be easily observed. Such animations may also be found in the public folder links provided in Appendix.

Here, we present a summary of the images produced during the project. Readers may refer to the links provided in Appendix for a repository of full set of images prepared during the project.

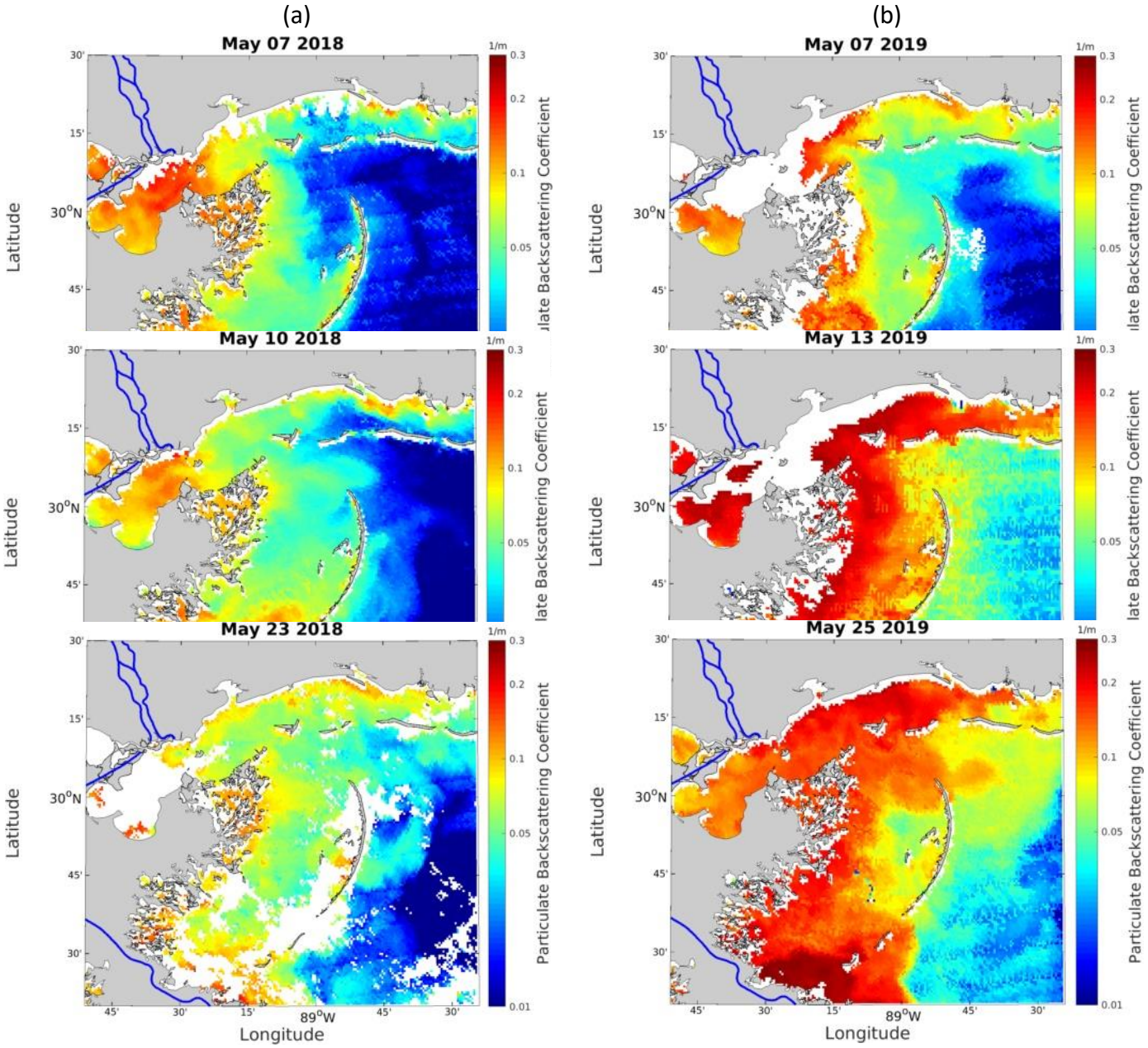

Figure 1. *Particulate backscattering (bb551) in the study area on (a) May 7, 2018 (b) May 7, 2019 (c) May 10, 2018 (d) May 13, 2019 (e) May 23, 2018 (f) May 25, 2019*

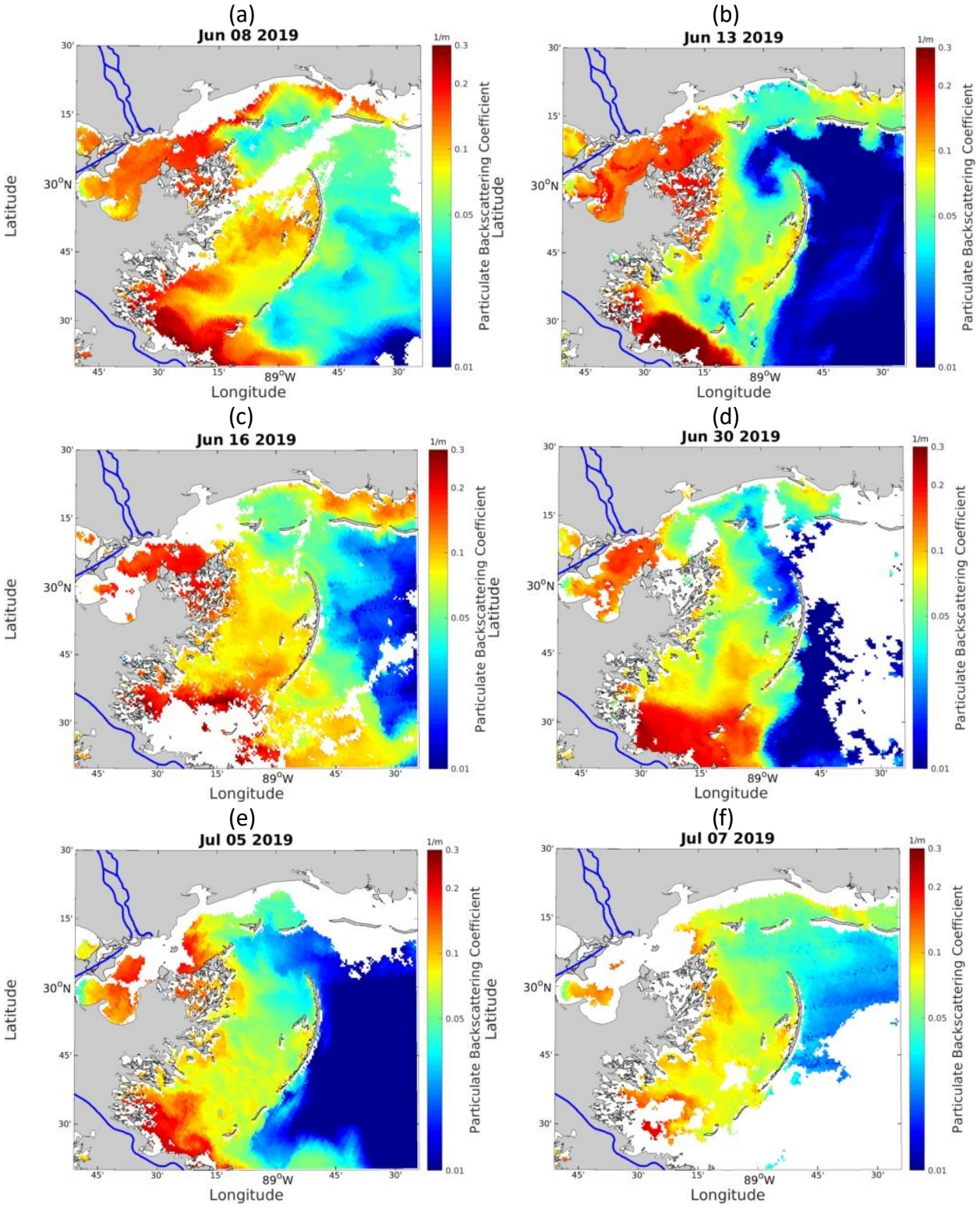
(a)
Jun 08 2019
(b)
Jun 13 2019
(c)
Jun 16 2019
(d)
Jun 30 2019
(e)
Jul 05 2019
(f)
Jul 07 2019
Latitude
Longitude
30°N
89°W
45'
30'
15'
1/m
0.3
0.2
0.1
0.05
0.01
Particulate Backscattering Coefficient
Particulate Backscattering Coefficient
Latitude

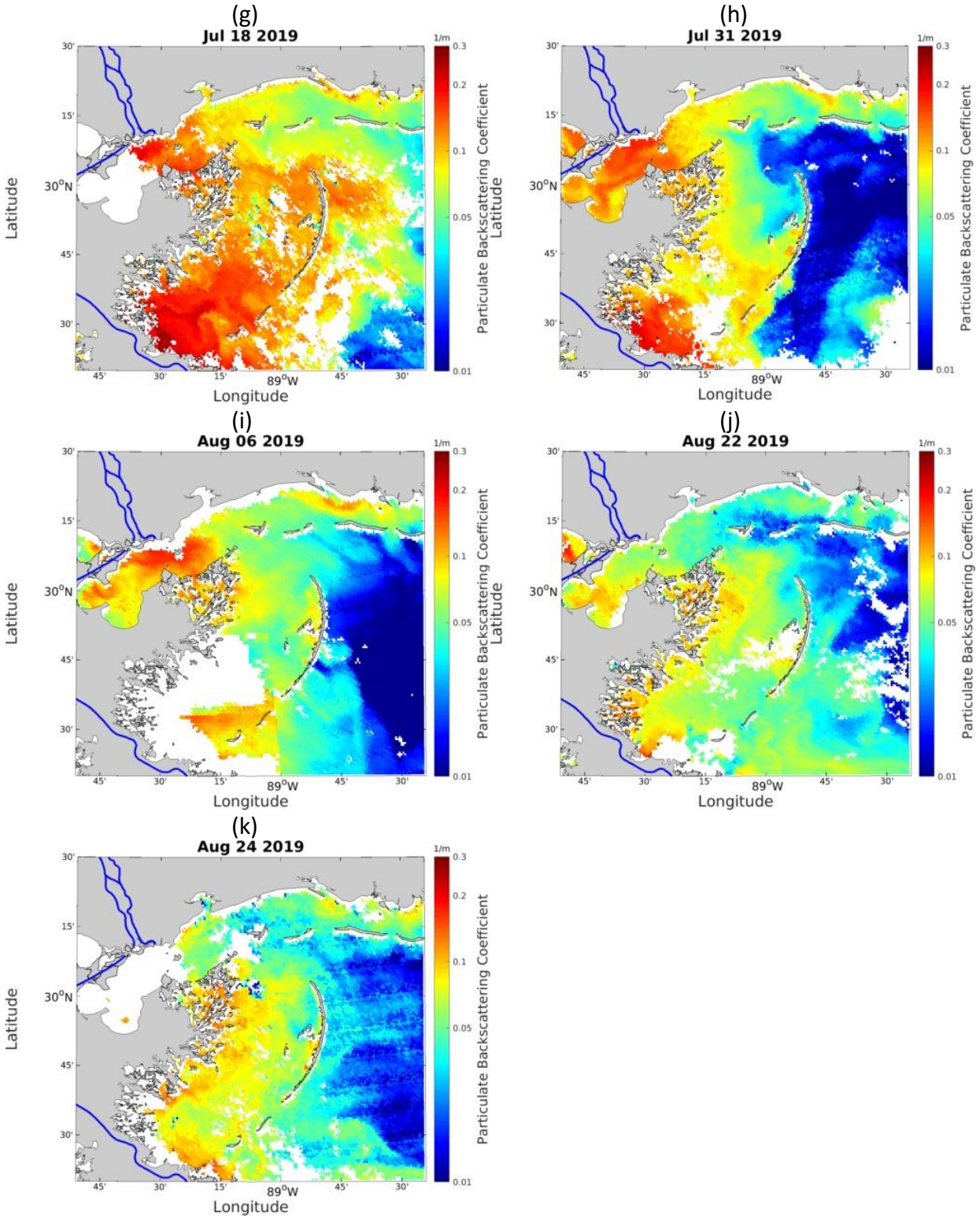

Figure 2. *Particulate backscattering (bb551) in the study area on (a) Jun. 8 (b) Jun. 13 (c) Jun. 16 (d) Jun. 30 (e) Jul. 05 (f) Jul. 07 (g) Jul. 18 (h) Jul. 31 (i) Aug. 6 (j) Aug. 22 (k) Aug. 24, 2019.*

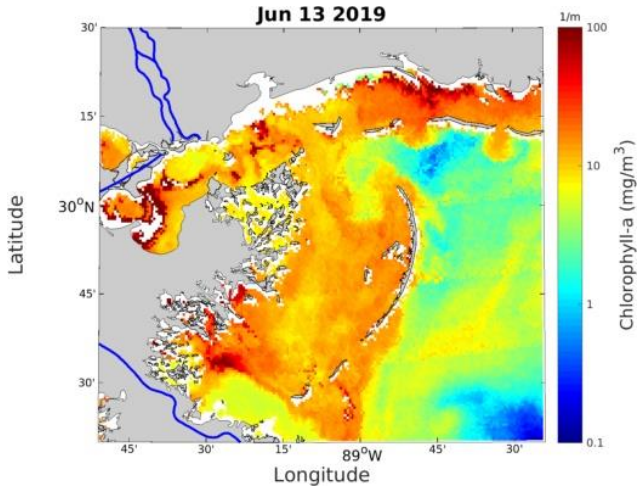

Figure 3. *Chlorophyll-a (chl-a) in the study area on June 13, 2019.*

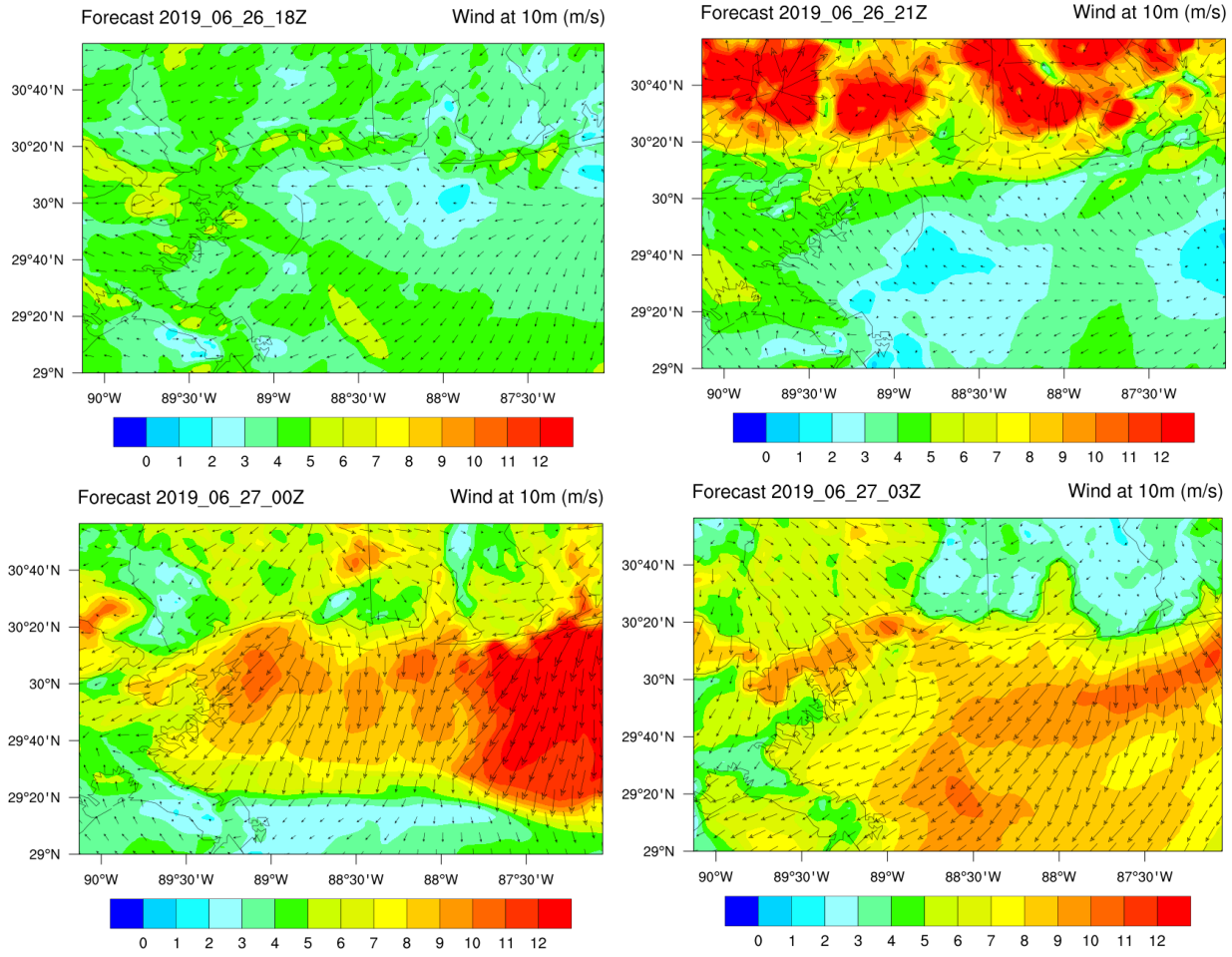

Figure 4. *Atmospheric model (WRF) results of forecast winds in June 2019, the colorbar indicates surface wind speed in m/s and the arrows indicate surface wind direction at 10 meter height.*

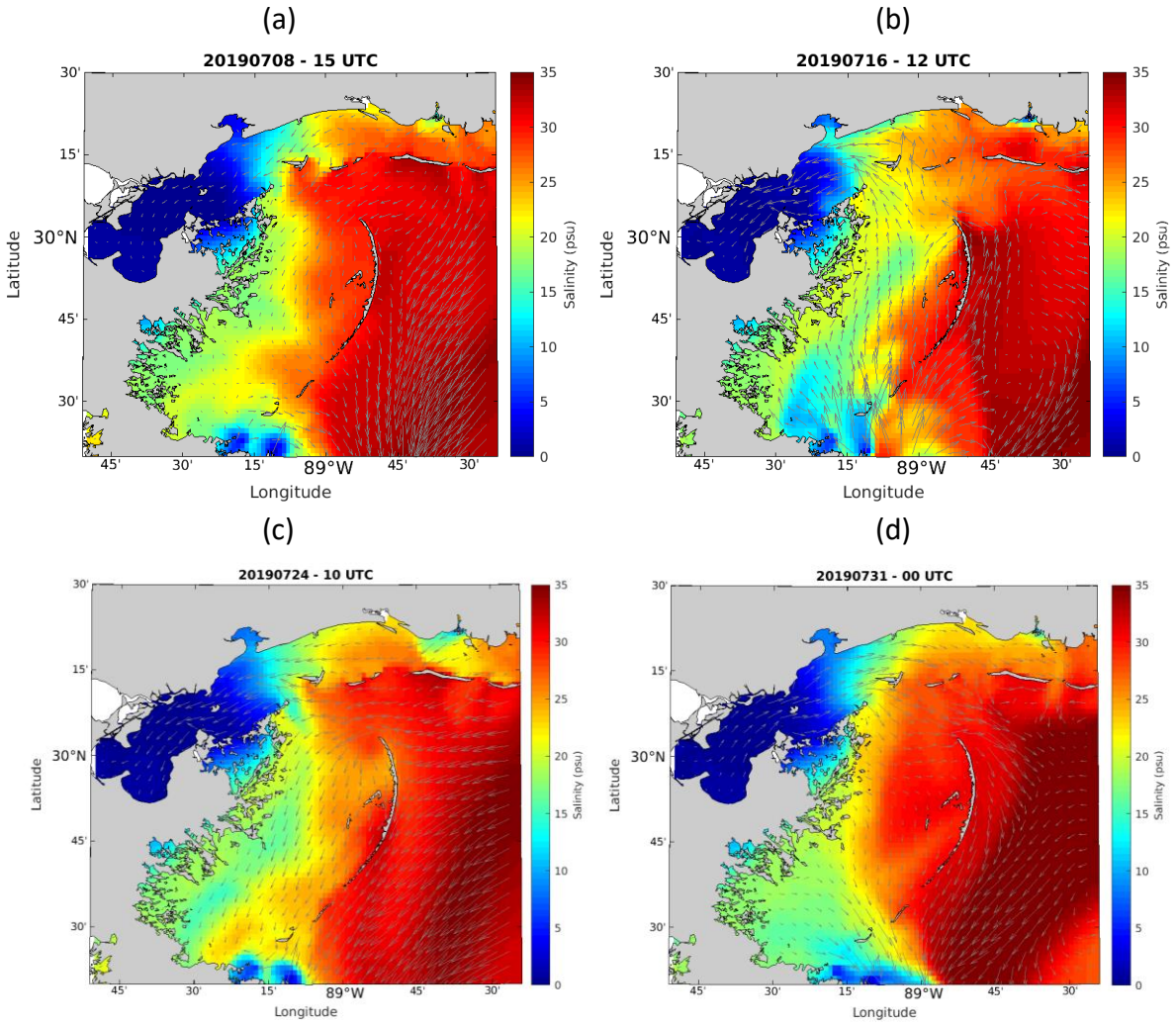

Figure 5. *Surface salinity and current distribution from NGOFS ocean modeling system over the study area during and after the 2019 Bonnet Carré spillway opening on (a) July 7, (b) July 16, (c) July 24, (d) July 31, 2019.*

References

[1] www.avl.class.noaa.gov/
[2] Werdell, P.J, Franz, B.A., Bailey, S.W., Feldman, G.C., et al. (2013). Generalized ocean color inversion model for retrieving marine inherent optical properties. Applied Optics 52, 2019-2037.
[3] Gordon, H.R., & Wang, M. (1994). Retrieval of water-leaving radiance and aerosol optical thickness over the oceans with Sea-WiFS: a preliminary algorithm. Applied Optics 33,443-52.
[4] Lee, Z. (2014). Update of the Quasi-Analytical Algorithm (QAA_v6). Available online: http://www.ioccg.org/groups/Software_OCA/QAA_v6_2014209.pdf (accessed on 19 November 2017).
[5] Lee, Z.; Carder, K.L.; Arnone, R.A. (2002). Deriving inherent optical properties from water color: A multiband quasi-analytical algorithm for optically deep waters. Appl. Opt., 41, 5755–5772.
[6] Qi, J. H., C. S. Chen, R. C. Beardsley, W. Perrie, G. W. Cowles, and Z. G. Lai (2009), An unstructured-grid finite-volume surface wave model (FVCOM-SWAVE): Implementation, validations and applications, Ocean Modelling, 28(1-3), 153-166, doi:10.1016/j.ocemod.2009.01.007.
[7] https://tidesandcurrents.noaa.gov/ofs/ngofs/ngofs_info.html
[8] https://opendap.co-ops.nos.noaa.gov/thredds/ngofs_catalog.html
[9] C. Skamarock *et al.*, "A Description of the Advanced Research WRF Version 3," 2008.

[10] S. G. Benjamin *et al.*, "A North American Hourly Assimilation and Model Forecast Cycle: The Rapid Refresh," *Mon. Weather Rev.*, vol. 144, no. 4, pp. 1669–1694, Apr. 2016.
[11] B. K. Blaylock, J. D. Horel, and S. T. Liston, "Cloud archiving and data mining of High-Resolution Rapid Refresh forecast model output," *Comput. Geosci.*, vol. 109, pp. 43–50, Dec. 2017.
[12] https://rapidrefresh.noaa.gov/hrrr/

Appendix

The images of satellite ocean color data, ocean model data and atmospheric model data were collected in an online repository and shared with other Bonnet Carré sampling project participants. Readers may reach to this repository and individual components from the following links:

	Inside USM-network link	Outside USM-network link
Main folder	http://10.14.4.54/~BCS_share/	http://131.95.1.37/~BCS_share/
Satellite ocean color data folder	http://10.14.4.54/~BCS_share/Satellite-Ocean-Color/	http://131.95.1.37/~BCS_share/Satellite-Ocean-Color/
Ocean model data folder	http://10.14.4.54/~BCS_share/CircModel/	http://131.95.1.37/~BCS_share/CircModel/
Atmospheric model data folder	http://10.14.4.54/~BCS_share/Wind/	http://131.95.1.37/~BCS_share/Wind/

Component 3: Fishery Resources

Component Lead Investigator: Zack Darnell
Co-PI: Chet Rakocinski

Blue Crabs

METHODS: Blue crabs were sampled during Summer 2019 at fixed stations throughout Mississippi Sound using crab traps. Stations consisted of a subset of the expanded water quality stations (1–4, 9, 12, and 15) and an additional station near Horn Island (30.25151°, -88.74350°), which is recognized as an important spawning area for blue crabs in Mississippi (Figure 1). During each sampling event, 5 traps were set at each station in a line running N-S, centered on the station location, with 200 m spacing between traps. Traps are baited with a 200–300 g of previously frozen menhaden and deployed for 48 h prior to retrieval. At the time of retrieval, crabs were sorted and counted by sex, maturity stage, and reproductive stage, and weighed for total crab biomass per trap.

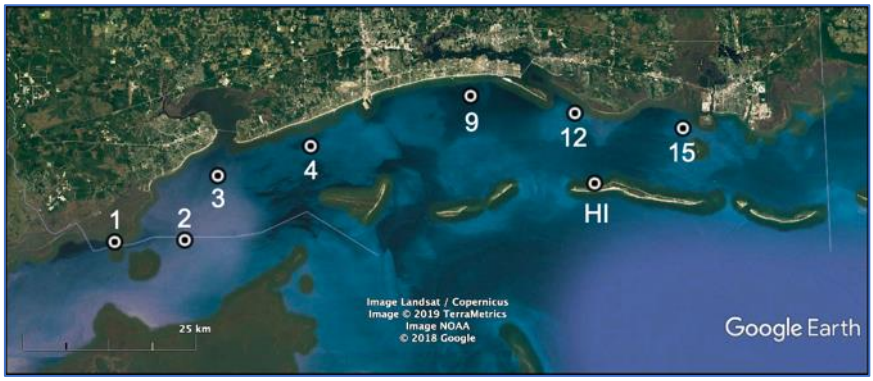

Figure 1. *Blue crab sampling locations in Mississippi Sound. Numbers correspond to expanded water quality station numbers. HI indicates the fixed station at Horn Island.*

Sampling for blue crabs took place June 26–28 (stations 9, 12, 15, and HI only), August 12–15 (all stations), and August 21–23 (stations 9, 12, 15, and HI only). During the June 26–28 and August 12–15 sampling events, a subset of crabs (1 per trap per station) were placed on ice and returned to the laboratory for analyses of two pathogenic disease agents. Hemolymph from a total of 46 blue crabs were collected to assess for infections of White Spot Syndrome Virus (WSSV) and the parasitic dinoflagellate *Hematodinium perezi.* Hemolymph was collected from base of swimming leg of each blue crab with a separate sterile tuberculin syringe. Data for WSSV was analyzed according to Durand and Lightner (2002), and those for *H. perezi* analyzed according to Nagle et al. (2009).

RESULTS: Sampling in June (26–28) focused on the eastern Mississippi Sound, with sampling occurring at stations 9, 12, 15, and Horn Island. Catch was highest at Horn Island, intermediate at station 12 (Bellefontaine) and 15 (Pascagoula), and lowest at station 9 (Biloxi) (Figure 2). It should be noted that DO at station 9 was low during sampling (1.7 ± 0.5 mg L^{-1}).which may account for the low catch. Catch at all stations consisted of >50% females, with ovigerous females present only at Horn Island.

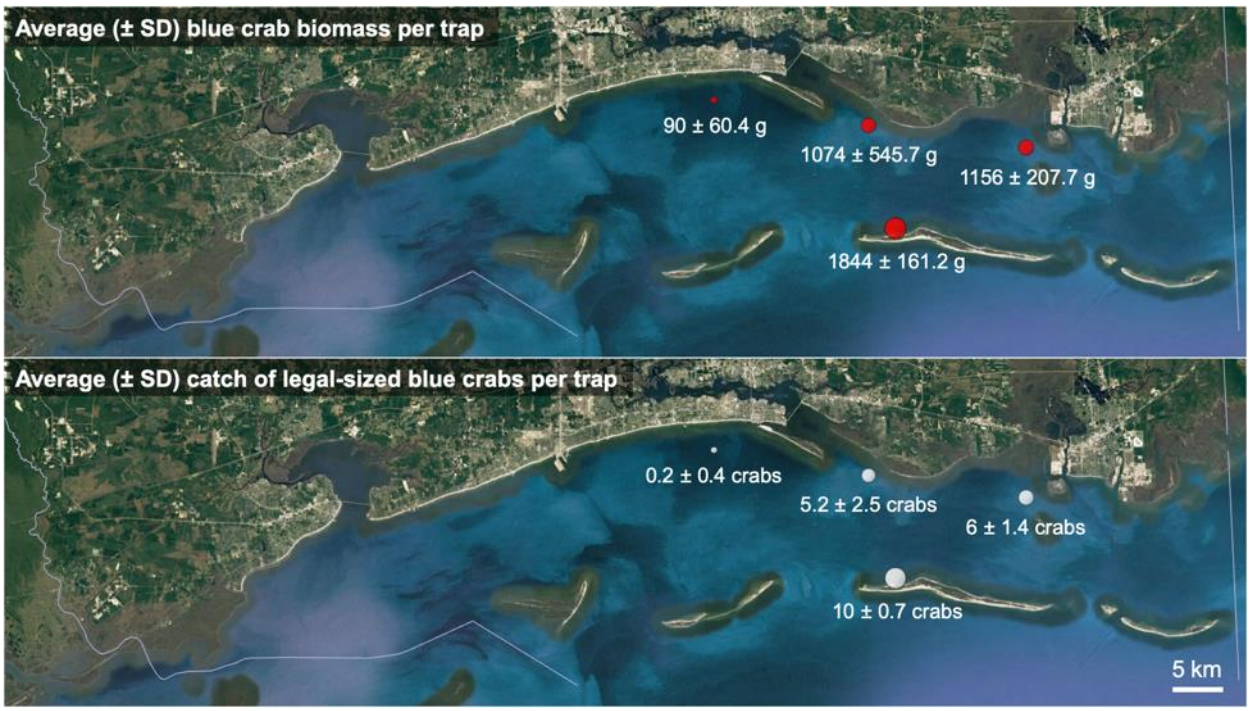

Figure 2. *Results of fishery-independent blue crab sampling in eastern Mississippi Sound on June 28, 2019. Symbol size is proportional to catch. Top panel shows average (± standard deviation) blue crab biomass caught in each trap. Bottom panel shows average (± standard deviation) number of legal-sized (>5 inches carapace width) blue crabs caught in each trap.*

Sampling in mid-August (12–15) spanned Mississippi Sound, with sampling occurring at stations 1, 2, 3, 4, 9, 12, annd 15. Due to weather delays, soak times for stations 12 and 15 were ~66 hrs, exceeded our target of 48 hrs. Catch was high in the far eastern and western portions of the sound and comparatively lower in the more central stations (Figure 3). Once again, DO at station 9 was quite low (2.63 ± 1.2 mg L^{-1}), and all crabs captured at station 9 were dead in the traps. With the exception of station 1 (31% female), the catch at the remaining stations consisted of >70% females. Ovigerous females were present at stations 2, 4, 12, and 15.

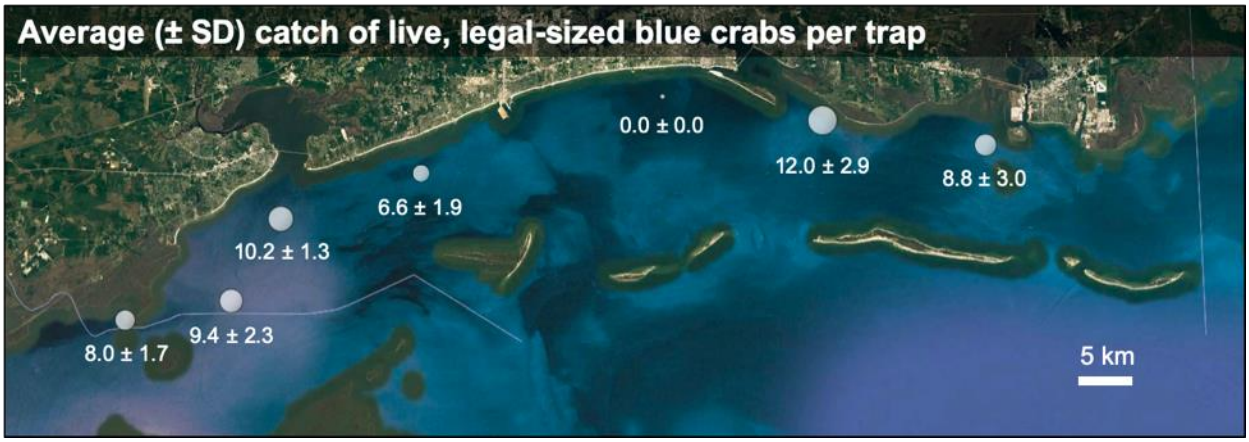

Figure 3. *Results of fishery-independent blue crab sampling in Mississippi Sound on August 14–15, 2019. Symbol size is proportional to catch.*

Sampling in late-August (21–23) focused on the eastern Mississippi Sound, with sampling occurring at stations 9, 12, 15, and Horn Island. Catch was relatively high at all station, including station 9, which was no longer experiencing low-DO conditions. The catch was composed of >80% females at all stations, with ovigerous females present at all stations. Comparisons of catch at stations 9, 12, 15, and Horn Island (the stations sampled multiple times) across are shown in Figure 4.

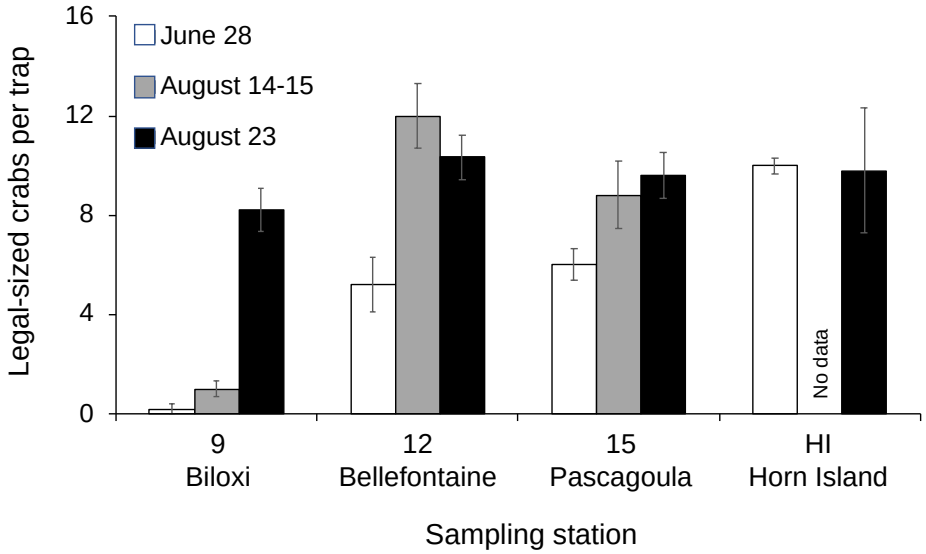

Figure 4. *Results of fishery-independent blue crab sampling in eastern Mississippi Sound. Five traps were set at each station, and catch is shown as average (± standard error) number of legal-sized (>5 inches carapace width) blue crabs caught in each trap. The top panel shows the location of each sampling station. Each station was sampled three times (June 28, August 14-15, and August 23), with the exception of station 20 (Horn Island), which was only sampled twice (June 28 and August 23).*

Pathogen analyses of samples collected on June 28 and August 14–15 2019 showed that all the crabs were infected with both agents. Most infections with WSSV were heavy enough to kill the crabs outright, and those with *H. perezi* could develop over time to a level high enough to kill all the crabs. The average levels of infections are shown in Figure 5, and comparisons between June and August could be made only for stations 12 and 15. In both those cases, the WSSV infections decreased with time and those with *H. perezi* increased. Penaeid shrimps typically die when WSSV levels reach 10^6, and the blue crab, which can tolerate more, can serve as a reservoir host capable of infecting penaeid populations feeding on dead infected crabs or on other crustaceans that had fed on the crabs. Intensity of the virus typically increases with time as the virus replicates. Experimental infections in the blue crab with *H. perezi* indicate that once a crab is inoculated with the agent, the infection will intensify, infective stages will develop, and the crab will ultimately die from the infection.

Our historical data on prevalence of infection for both agents from the same general area range from 1.8 – 18.0 % from 2011 to 2015 for WSSV and from 2.2 – 12.2 % for *H. perezi.* Infections from all stations and collections during the Bonnet Carré Spillway sampling project for both agents were 100 %. Historical data showed very few (7 of nearly 4,000 crabs) cases of both agents infecting the same individual as opposed to 100 % of the cases in the present samples. A representative crab from the present collection suggested

that it and probably others came from offshore of Mississippi Sound. This assumption was based on the presence of symbionts on the gills and carapace that require high salinity water to settle and develop, and, in one case, the infection lasted at least through a spawning generation period in that high salinity water. Presumably, all the collected crabs in our samples would have died from either of the agents after a short period. The Spillway opened twice (27 February until 11 April and 10 May until 22 July 2019) so exactly from where and when the crabs entered Mississippi Sound and when the crabs became infected are difficult to determine. Infections could not be tied to the distance from the Spillway, but the intensity of those with *H. perezi* seemed to be slightly more when closer to source of the discharged water. A continuation of monitoring would prove important in assessing mortality of the local blue crab population.

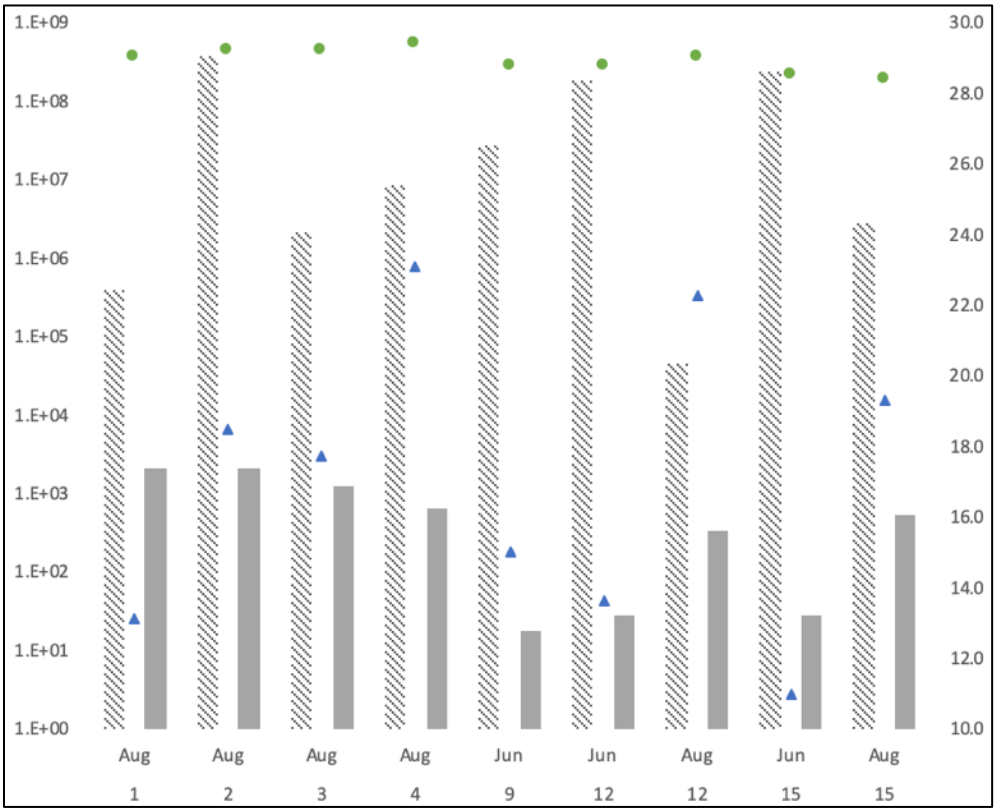

Figure 5. *Infections of White Spot Syndrome Virus (average WSSV copies/ng DNA) and* Hematodinium perezi *(average H. perezi/ng DNA) in the blue crab from Stations 1, 2, 3, 4, 12, and 15 off Mississippi coast in June and August 2019 relative to salinity in ppt (triangle) and temperature in degrees Centigrade (circle). X-axis shows months and stations sampled; left y-axis shows log of agents' copy numbers; and right y-axis shows values for both salinity and temperature during time of crabs' collection.*

Oysters

METHODS: In response to the prolonged opening of the Bonnet Carré spillway along with sustained massive freshwater discharge into Mississippi Sound well into the summer of 2019. Other surveys within the area indicated decimated local spawning stocks within the western Mississippi Sound (personal communication). Ecological factors known to influence oyster settlement include physical variables

including salinity and dissolved oxygen (DO), the presence of adult oysters (and other water borne cues), proximity of nearby sources of larvae coupled with the hydrodynamic transport process, substrate type, height and position (e.g., vertical) of the substrate, and the presence of refuge from predators. Variation in any or all of these factors will affect the chances for oyster reef recovery success.

A basic question relative to oyster reef maintenance and restoration is to what extent reefs depend on the supply of spat and on post-settlement processes affecting spat survival and growth. Depending on the relative contributions of local versus more remote sources of competent oyster larvae to an area, local decimation of adult spawning stock will have greater or lesser consequences for recovery of oyster reefs. Thus, resilience of the reefs depends critically on an uninterrupted supply of early oyster stages.

Accordingly, we initiated a spat settlement survey within seven key oyster reef areas (Figure 6), starting in July, 2019. Four settlement samplers (Figs. 7 and 8) consisting of concrete blocks, each housing two settlement plates are deployed at each site for four to five week periods. Both upper and lower surfaces of settlement plates are quantified. Lower surfaces situated close to bricks are also predation restricted.

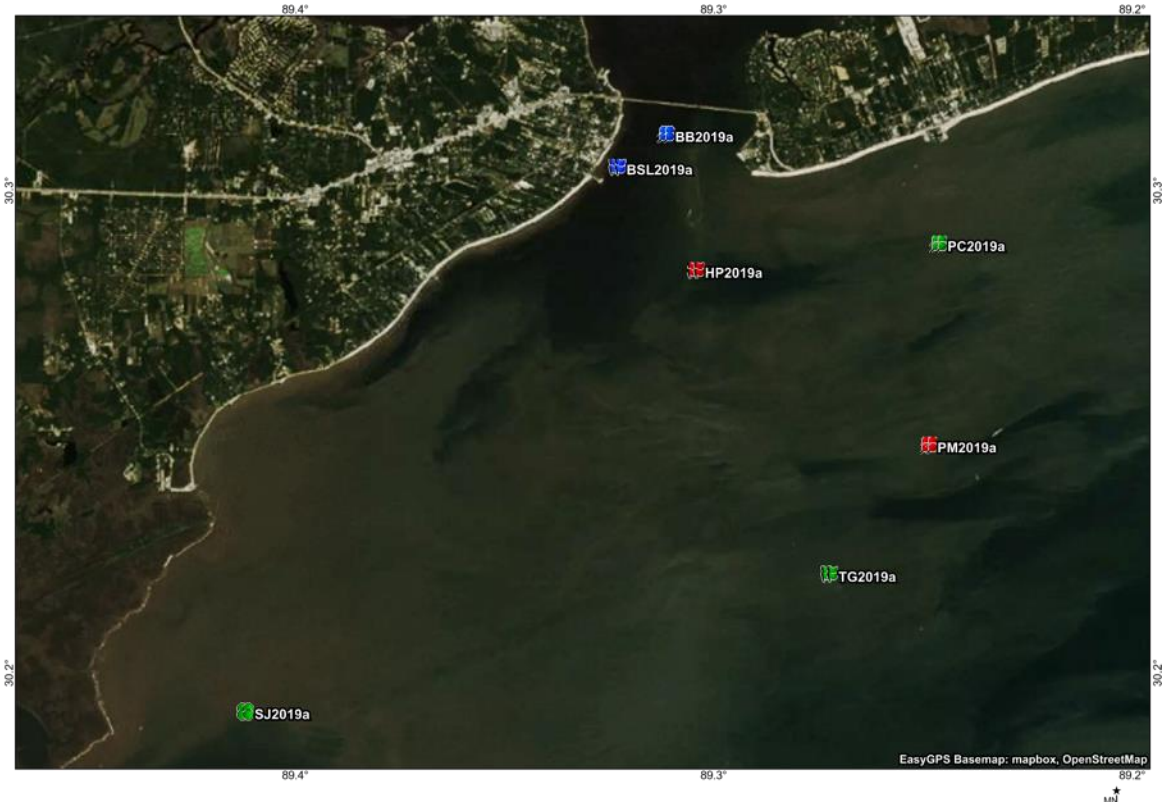

Figure 6. *Map of study sites where spat settlement samplers were deployed within oyster harvest areas throughout western Mississippi Sound in July and retrieved in August 2019 for MS DMR. Spat samplers consisting of concrete blocks with two 6 square-inch settlement plates affixed were deployed at four stations within each site. SJ – Saint Joe Reef; BSL – Bay St. Louis Reef; BB – Between Bridges; HP – Henderson Point Reef; PC – Pass Christian Reef; PM – Pass Marianne Reef; TG – Telegraph Reef.*

Figure 7. *Deployment of settlement samplers in July 2019.*

Figure 8. *Retrieval of spat settlement sampler in August 2019.*

Recruitment metrics routinely obtained from settlement plates include abundances of new (< 2 mm) and later spat, mean spat size, maximum spat size (proxy of growth), numbers of spat scars (proxy of mortality /predation), percent spat cover, percent barnacle cover (proxy of competitors). Physical and habitat measurements are obtained in conjunction with spat settlement and growth data, including salinity, temperature, dissolved oxygen, depth, and turbidity. Fortuitously, we had conducted a comparable study supported by MBRACE within some of the same areas in 2018, when we conducted a focused spat settlement study within the western Mississippi Sound harvest area at 8 sites. These samples have been processed.

The first set of settlement samplers was deployed in July and retrieved in August. One of the MBRACE 2018 sample periods closely matched this period of deployment. General GPS locations and physical data associated with these events are provided in the associated metafile. Surface salinities ranged from 1.3 to 5.0 across the seven sites in July; and ranged higher, from 1.5 to 11.1 upon retrieval in August. Casual observations of settlement plates upon retrieval showed no evidence of oyster spat, although laboratory inspections would be needed to confirm that impression. By comparison, retrieval of settlement plates from the same region at the same time of year bore obvious signs of spat settlement.

Funding for this project was terminated on August 31, 2019, before there was time to work up the set of settlement samples from August. Recovered settlement plates have been archived by freezing and remain unquantified. Two more subsequent sets of settlement plates from the same sites have also been taken in September and October, due to the importance of knowing whether early recruitment of oysters is now limited in western Mississippi Sound. Field work expenses for these two additional sets were supported by MBRACE. In addition, the workup of the second set of settlement plates retrieved in September is being supported by MBRACE. The first and third sets will remain archived pending funding to work them up. These samples are important for determining recruitment limitation of oysters in western Mississippi Sound at a time of catastrophic loss of adult oyster stock. Out superficial impression during retrieval of settlement

samplers during all three periods in August, September, and October was that spat settlement was not apparent, especially in comparison to the previous year.

References

Durand, S. V., Lightner, D. V, 2002. Quantitative real time PCR for the measurement of white spot syndrome virus in shrimp. Journal of Fish Diseases 25: 381–389.

Nagle, L., Place, A.R., Schott, E.J., Jagus, R., Messick, G., Pitula, J.S., 2009. Real-time PCR-based assay for quantitative detection of *Hematodinium* sp. in the blue crab *Callinectes sapidus*. Diseases of Aquatic Organisms 84: 79–87.

Component 4: Data Synthesis

Component Lead Investigator: Robert Leaf
Co-PI: Scott Milroy

All data collected as part of this project were subject to standard QA-QC procedures by the collecting investigator. Those data and associated metadata were then accumulated and centralized in a web-based repository. This repository serves to organize and describe the products derived from environmental and biological sampling performed by USM researchers to aid in determining the extent of impacts from freshwater in the Mississippi Sound associated with the opening of the Bonnet Carré Spillway in 2019.

Data, Meta Data, and a Data and Meta Data Summary directories are located in a Google Drive Repository that can be accessed here: https://drive.google.com/open?id=1cKUzfGNFURqCZlmyQ4ux9Hp6qERfHsKn The .md file is a living document to describe the structure of the repository.

- Data (https://drive.google.com/open?id=1n8lHUhrLVZA-hFnV3S2uY-N-GgnLxVhb):
    - Living Marine Resources (Fishes and Invertebrates)
    - Secchi
    - Sonde/YSI Envrionmental Sampling
    - Vibrio and Bacterial DNA
    - Nutrient and Isotopes
    - Phytoplankton
    - Shape Files directory includes high resolution .shp files for the region
    - Station list "BC_STATIONS.csv" contains the decimal degree locations for all fixed sampling stations
- Meta Data (https://drive.google.com/open?id=1mQgwByIFQ3WX8w6f0Uvhks65q8voBBZT):
    - .xlsx files that describe the structure of the data collected during the project
- Data and Meta Data Summary (https://drive.google.com/open?id=1wWP_qha0Y2ENYcSMB_KAFF2DCaNGwVOK):
    - .html files that summarize in tables and figures the station-, spatial-, and temporal-specific patterns in the collected data.